

**Part 1: Zonal gradients in phosphorus and nitrogen acquisition and stress revealed by metaproteomes of *Prochlorococcus* and *Synechococcus***

Claire Mahaffey<sup>1\*</sup>; Noelle A. Held<sup>2,3,4\*</sup>; Korinne Kunde<sup>5,6</sup>; Clare Davis<sup>1†</sup>; Neil Wyatt<sup>6</sup>; E. Matthew R. McIlvin<sup>2</sup>,  
5 Malcolm S. Woodward<sup>7</sup>; Lewis Wrightson<sup>1</sup>; Alessandro Tagliabue<sup>1</sup>; Maeve C. Lohan<sup>6</sup>; Mak Saito<sup>2</sup>

**Deleted:** Liverpool

<sup>1</sup>Earth, Ocean and Ecological Sciences, University of Liverpool, [Liverpool](#), UK L69 3BX

<sup>2</sup>Department of Marine Chemistry and Geochemistry, Woods Hole Oceanographic Institution, Woods Hole, USA

<sup>10</sup>Department of Environmental Systems Science, ETH Zürich, Zürich, Switzerland

<sup>4</sup>Department of Biological Sciences, Marine & Environmental Biology Section, University of Southern California, Los Angeles, CA, USA

<sup>5</sup>School of Oceanography, University of Washington, Seattle, USA

<sup>6</sup>Ocean and Earth Sciences, University of Southampton, [Southampton](#), UK SO14 3ZH

<sup>15</sup>7Plymouth Marine Laboratory, [Plymouth](#), UK PL1 3DH

<sup>†</sup>Current address: Springer Nature, London, UK

\*Joint first authors and corresponding authors: [mahaffey@liverpool.ac.uk](mailto:mahaffey@liverpool.ac.uk), [nheld@usc.edu](mailto:nheld@usc.edu)

**20 Research Article**

**Short summary**

Ocean primary production helps regulate climate through carbon cycling. The magnitude of this process is governed by the availability of nutrients, such as nitrogen, phosphorus, iron and zinc. Here, we analyse zonal gradients in microbial nutrient acquisition strategies and potential nutrient limitation in the surface subtropical Atlantic Ocean to determine how changes in nutrient resources impact marine primary productivity. Nutrient and trace metal availability, biological activity, and protein biomarker abundance are determined to infer phosphorus, nitrogen and trace metal acquisition and metabolism in two dominant picocyanobacteria, *Prochlorococcus* and *Synechococcus*. We find phosphorus stress prevails for both *Prochlorococcus* and *Synechococcus* in the western Atlantic, but that *Prochlorococcus* becomes increasingly nitrogen, iron, zinc and cobalamin stressed in the east with coincidently lower phosphorus biomarker proteins, indicating a switch in nutrient status across the transect. Our findings provide species and ecotype level insights into nutrient acquisition and metabolism in the ocean, combining biogeochemical and biological rate measurements with discovery and targeted proteomics to understand how microbial metabolism will respond to a changing climate.

**Deleted:**

**Deleted:** the nutrient

**Deleted:** resources

**Deleted:** Alongside measurements of states and rates, discovery and targeted proteomics can be powerful tools in

**Deleted:** enhancing

**Deleted:** understanding

**Deleted:** Marine primary production supports marine ecosystems and helps to regulate climate through carbon cycling. The magnitude of productivity is underpinned by the availability of nutrient resources, such as nitrogen, phosphorus, iron, zinc and cobalt. Natural variation alongside anthropogenic activity has the potential to alter both the absolute and relative amount of nutrients available to marine microbes. To fully understand the impact of the evolving nutrient resource environment on marine primary productivity, we need to know how different marine microbes acquire nutrients, and which nutrients have the potential to limit productivity. In this study, we used zonal gradients in nutrients, trace metals, biological activity and protein biomarkers representing phosphorus, nitrogen and trace metal acquisition and metabolism to better understand how two dominant picocyanobacteria, *Prochlorococcus* and *Synechococcus*, acquire nutrient resources in the surface subtropical ocean. Our suite of measurements agree on the occurrence of phosphorus stress for both *Prochlorococcus* and *Synechococcus* in the western Atlantic, but increases in proteins representing nitrogen, iron, zinc and cobalamin metabolism in *Prochlorococcus* in the east where phosphorus biomarker proteins are lower indicates a switch in the nutrient resources controlling the growth of *Prochlorococcus* across the transect. Our study highlights the power of a combined discovery and targeted proteomics approach in providing species and even ecotype level information on nutrient acquisition and metabolism, which alongside measurements of states and rates, can be powerful tools in enhancing understanding of microbe metabolism in a changing climate.

**Deleted:** However

**Deleted:** , t

**Deleted:** changes

**Deleted:** environment

**Commented [MS1]:** Adding some of the big picture zonal observations if space. Left out N since more complicated (double peak in N+N and N fixation trends in the middle/east) and since P is the emphasis here.

between strains. Together our findings suggest a basin-scale transition from phosphorus stress in picocyanobacteria in the west to nitrogen stress in the east.

## 95 1. Introduction

Marine phytoplankton have an important role in biogeochemical cycles, supporting ecosystems and regulating climate. Global net primary productivity (NPP) is underpinned by availability of key nutrient resources, such as nitrogen (N), phosphorus (P), iron (Fe) and zinc (Zn) and others. In the subtropical open ocean, surface nutrient concentrations are chronically low and often limit NPP. Enhanced stratification, induced by ocean warming,

100 alongside changes to natural and anthropogenic supply of fixed N (Chien et al., 2016; Kim et al., 2014; Wrightson and Tagliabue, 2020), P (Barkley et al., 2019) or Fe (Liu et al., 2022) to the global ocean are likely to perturb the magnitude and ratio at which nutrients are supplied to phytoplankton (Peñuelas et al., 2013), potentially expanding or intensifying nutrient limited ocean regions (Bopp et al., 2013; Chien et al., 2016; Lapointe et al., 2021). Detecting and understanding how nutrients regulate phytoplankton distribution, growth 105 and activity is key to estimating the magnitude and direction of contemporary and future NPP, reducing uncertainty and assessing risks to ecosystem services (Tagliabue et al., 2021).

The nutrient that limits phytoplankton growth can be identified by adding single or multiple nutrients to seawater and measuring phytoplankton growth or other properties over time (Browning and Moore, 2023; Mahaffey et al.,

110 2014; Mills et al., 2004; Moore et al., 2008). In addition, advances in 'omics' have enabled identification of protein biomarkers related to nutrient acquisition of stress in marine phytoplankton (Chappell et al., 2012; Hawco et al., 2020; Held et al., 2020, 2025; Rouco et al., 2018; Saito et al., 2014, 2015; Ustick et al., 2021). Identifying regions of N and/or Fe stress is straightforward (Browning and Moore, 2023) but detecting P stress can be more challenging. Systems-level interpretation of incubation results and biomarker abundances is needed to 115 disentangle the effects of nutrient biogeochemistry and biological plasticity/activity. For instance, in low-phosphate regions dominated by the ecologically important picocyanobacteria, *Prochlorococcus*, phosphate addition experiments imply a lack of P stress, whereas genomic data identifies large areas of P stress for *Prochlorococcus* (Browning and Moore, 2023). This mismatch may be due to the flexibility in P acquisition strategies demonstrated by key marine phytoplankton (Duhamel et al., 2021; Martínez et al., 2012; Martiny et al.,

120 2006, 2009; Moore et al., 2005; Ostrowski et al., 2010; Scanlan et al., 1993; Tetu et al., 2009). In addition, phosphate limited phytoplankton can deploy an array of strategies to acquire alternative sources of P from dissolved organic phosphorus (DOP) including esters (Sebastian and Ammerman, 2009; Tetu et al., 2009), polyphosphate (Moore et al., 2005), phosphite (Martínez et al., 2012) and phosphonate (Ilikchyan et al., 2010) or substituting P-rich lipids with P-free alternatives (Van Mooy et al., 2009). A hydrolytic metalloenzyme group,

125 alkaline phosphatases, are responsible for cleaving P from esters (Hoppe, 2003). Enhanced activity of alkaline phosphatase (AP) has been used as an indicator of P limitation (Mahaffey et al., 2014; Su et al., 2023) although the substrate specificity (Srivastava et al., 2021), cellular localisation (Luo et al., 2009), AP allocation between ecotypes (Moore et al., 2005), uncertainty in the contribution of different phytoplankton groups to total enzyme activity (Held et al., 2025; companion study to this manuscript)) and lack of knowledge on the efficiency of

**Deleted:** Ocean warming alongside changes to the natural and anthropogenic supply of key nutrient resources such as nitrogen, phosphorus and trace metals is predicted to alter the magnitude and stoichiometry of nutrients that are essential for maintaining ocean productivity. To improve our ability to predict how marine microbes will respond to a changing nutrient environment, we need to better understand how natural assemblages of marine microbes acquire nutrients. We combined observations of natural zonal gradients across the North Atlantic subtropical gyre of the state of nutrient resources and microbial proteomes with biological activity rates, to investigate the factors influencing the distributions and nutrient acquisition strategies of the dominant picocyanobacteria, *Prochlorococcus* and *Synechococcus*. Dissolved organic phosphorus decreased by more than a factor of two moving westward, while phosphate increased eastward with eastern boundary upwelling and dissolved iron increased westward with dust deposition. Picocyanobacterial populations diverged across the zonal transect with *Prochlorococcus* increasing in abundance westward, while maintaining numerical dominance throughout, and while *Synechococcus* increased in abundance in the westward basin, implying a low phosphorus niche. We analysed the zonal distribution of protein biomarkers representing phosphorus (PstS, PhoA, PhoX), nitrogen (P-II, UrtA, AmtB) and trace metal metabolism (related to iron, zinc and cobalt) alongside the response of phosphorus protein biomarkers to the addition of dissolved organic phosphorus with iron or zinc within incubation experiments. Rates of alkaline phosphatase alongside phosphorus protein biomarkers concur on more intense phosphorus stress in the western compared to the eastern subtropical Atlantic for both picocyanobacteria. Protein biomarkers for nitrogen, iron, zinc and cobalamin in *Prochlorococcus* increased to the east where phosphorus protein biomarkers were lower, indicating a transition to N stress and increasing role of trace metal resources in controlling *Prochlorococcus* growth. We use the diverging zonal patterns in protein biomarkers, alongside the response of *Prochlorococcus* and *Synechococcus* to nutrient addition, to p ... [1]

**Deleted:** .

**Deleted:** play a critical role in elemental cycling,

**Deleted:** many

**Deleted:** Over large ocean regions, such as subtropical gyres

**Deleted:** concentrations of these

**Deleted:** key

**Deleted:** s

**Deleted:** in surface waters

**Deleted:** limiting

**Deleted:** Evaluating the prevalence and impact of limitation by one or more nutrients on the growth and activity of phytoplankton ... [2]

**Deleted:** A

**Deleted:** analysis of the genetic or protein makeup of marine phytoplankton to identify proteins indicative of nutrient acqui ... [3]

**Deleted:** :

**Deleted:** is

**Formatted:** Strikethrough

**Formatted:** Strikethrough

**Commented [NH3]:** I'm a little worried about this statement because it implies that there is a lot of P stress and that it is diff ... [4]

**Deleted:** .

**Deleted:** I

**Deleted:** the addition of phosphate would imply

**Deleted:** . However, identifying regions of P stress was more challenging, with disagreement between results from nutrient ... [5]

**Deleted:** in the low-phosphate ocean regions

**Formatted:** Font: Italic

**Deleted:** Under phosphate scarcity,

**Deleted:** .

**Deleted:** submitted

255 different AP enzymes raises uncertainties. Collectively, the flexibility in P acquisition strategies, as well as the perceived ability of *Prochlorococcus* to readily satisfy their P demands at ultra-low concentrations of phosphate (Lomas et al., 2014) has led to the idea that *Prochlorococcus* evade nutrient stress, particularly by remodelling their proteomes.

**Deleted:** uncertainties in its applicability.

260 Comparing the physiological response of two ecologically important picocyanobacteria, *Prochlorococcus* and *Synechococcus*, to P stress demonstrates the complexity of deciphering resource limitation in mixed populations, between species, or even between strains of the same species. *Synechococcus* possess genes encoding a high affinity periplasmic phosphate binding protein (pstS) and transport system (pstABC), as well as genes encoding proteins essential for accessing organic P via alkaline phosphatase (phoA) and phosphonatase (phnC, D, E,

**Deleted:** for

265 (Moore et al., 2005; Scanlan et al., 1993; Tetu et al., 2009). When phosphate is scarce, *Synechococcus* has been shown to upregulate pstS, pstABC and phoA (Moore et al., 2005; Tetu et al., 2009), the regulator gene ptrA (Ostrowski et al., 2010) and the recent described high affinity AP gene psip1 (in clade III only, Torcello-Requena et al., 2024), with a measurable increase in AP activity (Moore et al., 2005, Torcello-Requena et al., 2024), implying that expression of these genes is indicative of P stress (Moore et al., 2005, Torcello-Requena et al., 2024).

**Deleted:** for

270 2024). However, clade specific variations in response to phosphate limitation have been observed *in situ* (Sohm et al., 2016, Torcello-Requena et al. 2024) and in culture (Moore et al., 2005). While *Prochlorococcus* also possesses pstS and pstABC and has been shown to upregulate these genes alongside phoA under phosphate deplete conditions (Martiny et al., 2006), strain specific variations in its ability to access organic P also exist. For example, while the two most prevalent high light (HL) clades, MED4 (HL1) and MIT9312 (HLII) can grow

275 solely on phosphate, MED4 grows on a wider range of organic P compounds, possess a high affinity AP (psip1, Torcello-Requena et al., 2024) and dramatically increases AP activity when P starved compared to MIT9312 (Moore et al., 2005).

**Deleted:** starvation

In addition to species and clade specific responses across the microbial realm, AP enzymes are dependent on a metal co-factor, with Zn and/or cobalt (Co) required for the protein PhoA (Coleman, 1992) and Fe and

**Formatted:** Font: Not Italic

**Formatted:** Indent: First line: 1.27 cm

**Formatted:** Font: Not Italic

280 calcium for the proteins PhoX and PhoD (Rodriguez et al., 2014; Yong et al., 2014) and Psip1 (Torcello-Requena et al., 2024). Although 130 the active sites of PhoA and PhoX in marine microbes have yet to be biochemically characterised, their metal requirements have been estimated assuming they are like the model organism, Escherichia coli and based on supporting evidence that the enzymes respond to the metals that they are expected to contain (Cox and Saito, 2013; Mikhaylina et al., 2022; Ostrowski et al., 2010). However, homology-based

**Formatted:** Font: Not Italic

**Formatted:** Font: 11 pt, Not Italic

**Formatted:** Font: Not Italic

**Formatted:** Font: Not Italic

**Formatted:** Font: Not Italic

285 annotation of enzymes is challenging and therefore the annotations herein should be considered putative. The trace-metal content of these proteins creates the potential for trace metals to control P acquisition via regulation of AP activity leading to Fe-P or Zn-P co-limitation (Browning et al., 2017; Duhamel et al., 2021; Held et al., 2025; Mahaffey et al., 2014). Observations of an accelerating stoichiometry of Co in the western North Atlantic has led to hypotheses for the potential for Co use in oceanic alkaline phosphatases too (Held et al., 2025; Jakuba et al., 2008; Saito et al., 2017). In culture studies, *Prochlorococcus* and *Synechococcus* have been shown to have absolute requirements for Co but not Zn under replete P conditions (Hawco et al., 2020; Saito et al., 2002; Sunda and Huntsman, 1995) but *Synechococcus* benefits from available Zn to produce AP under P scarcity (Cox and

**Deleted:** In addition to species and clade specific responses across the microbial realm, AP enzymes are dependent on a metal co-factor, with Zn and/or cobalt (Co) required for the protein PhoA (Coleman, 1992) and Fe and calcium for the proteins PhoX and PhoD (Rodriguez et al., 2014, Yong et al., 2014). Although the active sites of PhoA and PhoX in marine microbes have yet to be characterised, their metal requirements have been estimated assuming they are like the model organism, *Escherichia coli*. This

**Deleted:** dependency

**Deleted:** on

**Deleted:** and

**Deleted:** thus

Saito, 2013). Thus, knowledge of the phytoplankton community structure, alongside their nutritional preferences and enzyme characteristics is key in deciphering nutrient limitation in the ocean.

This study measures the biological response to nutrient transitions in the North

Atlantic Gyre. Here, the Western basin is heavily influenced by Saharan aeolian dust (Jickells, 1999), while the eastern basin borders the upwelling system off northwest Africa (Menna et al., 2015). Both upwelling and dust deliver scarce resources to the region, creating strong gradients in nutrients and trace metals (Gross et al., 2015; B15 Kunde et al., 2019; Reynolds et al., 2014; Sebastián et al., 2004) influencing productivity (Moore et al., 2008). DOP dynamics (Liang et al., 2022) and marine dinitrogen ( $N_2$ ) fixation (Moore et al., 2009). Here, we exploit these strong natural gradients in nutrient and trace metal resources and biological activity to investigate nutrient acquisition strategies of natural assemblages of *Prochlorococcus* and *Synechococcus*.

Alongside measurements of biogeochemical states, specifically nutrients, dissolved iron, zinc, cobalt and DOP and biological rates, including AP activity and  $N_2$  fixation, we investigated biological activity with non-targeted metaproteomics and quantitative targeted proteomics of the high affinity phosphate binding protein, PstS, and two alkaline phosphatases, PhoA and PhoX in *Prochlorococcus* and *Synechococcus* (Table 1). From the non-targeted metaproteomics analyses we specifically focus on proteins indicative of N acquisition (P-II, UrtA, AmtB) and proteins involved in iron (ferredoxin), zinc (zinc peptidase and transporter) and B<sub>12</sub> (cobalamin synthetase) metabolism (Table 1). This allowed us to firstly investigate the potential for *Prochlorococcus* and *Synechococcus* to be phosphorus-stressed in the subtropical Atlantic, challenging the view that avoidance of P limitation and hypothesised zonal gradients in proteins would reflect nutrient stress. We also assessed the potential for N, Fe and Zn to control the zonal distribution of *Prochlorococcus* and *Synechococcus*. Secondly, we assessed the potential for P acquisition to be regulated by the availability of DOP, Fe and Zn or Co. We hypothesised that the distribution of PhoA and PhoX would be reflected in rates of AP and alongside Fe and Zn, the limiting trace metal. We augmented *in-situ* sampling with nutrient bioassays, complimentary to those reported by Held et al., 2025 (companion manuscript), to further assess the potential for DOP substrate, alongside metals Fe and Zn to regulate AP activity and applied a quantitative proteomic approach targeting PstS, PhoA and PhoX only. Finally, we critically assessed our different approaches to delineate nutrient controls of the distribution and B35 physiological strategies of *Prochlorococcus* and *Synechococcus*, highlighting the nuanced insights gained when bringing together biogeochemical measurements alongside 'omics (Saito et al., 2024).

Table 1. Summary of the proteins targeted by metaproteome (all) and quantitative (\*) protein analysis including their function and known characteristics.

Protein name or family	Function and reported characteristics
PstS*	Periplasmic phosphate-binding protein. Induced under P-limiting conditions
PhoA*	Alkaline phosphatase: cleaves phosphorus from organic compounds. Zinc metalloenzyme Induced under P-limiting conditions
PhoX*	Alkaline phosphatase: cleaves phosphorus from organic compounds. Iron metalloenzyme. Regulation unknown
P-II	Nitrogen regulatory protein. Indirectly controls the transcription of glutamine synthetase gene <i>glnA</i> .
AmtB	Ammonium transporter channel. Transmembrane
UrtA	An ABC-type, high-affinity urea permease. Substrate binding protein

Ferredoxin	Iron metalloenzyme. Regulated by iron, more abundant under high iron conditions.
Zinc peptidase	Zinc metalloenzyme. Involved in proteolysis at the plasma membrane
Zinc transporter	Zinc metalloenzyme. ABC transporter, ATP-binding protein
Cobalamin synthetase	Cobalt metalloenzyme. Synthesis of cobalamin (vitamin B <sub>12</sub> )

## 355 2 Materials and methods

### 2.1 Sample collection from surface waters

Samples were collected on a zonal transect between Guadeloupe and Tenerife at approx. ~22°N between 26<sup>th</sup> June and 12<sup>th</sup> August 2017 onboard the *RRS James Cook* (JC150, Fig. 1a). Sea surface temperature (SST) was measured via the underway seawater system using Seabird sensors. Using a trace-metal clean towed FISH and a

360 Teflon diaphragm pump (Almatec A-15), seawater samples were collected every 2 h, at a resolution of ~ 25 km, from ~ 3 m below the surface (Fig. 1a), with seawater flow terminating into a class-100 clean air-laboratory.

### 2.2 Biogeochemical states and rates

Using unfiltered seawater samples from the towed FISH, concentrations of nitrate plus nitrite (Brewer and Riley, 365 1965), phosphate (Kirkwood 1989) and ammonium (Jones, 1991) were analysed onboard according to GO-SHIP nutrient protocols (Becker et al., 2020). Using filtered seawater from the towed FISH (Sartobran, Sartorius, 0.8/0.2 µm polyethersulfone membrane), concentrations of dissolved iron (Kunde et al., 2019) were measured onboard while concentrations of dissolved zinc (Nowicki et al., 1994) were determined at the University of Southampton. Concentrations of DOP were determined at the University of Liverpool using a modified version 370 of (Lomas et al., 2010) as described by (Davis et al., 2019). Using unfiltered seawater from the towed FISH, rates of alkaline phosphatase were determined onboard every 4 h or ~ 50 km; Davis et al., 2019). *Prochlorococcus*, *Synechococcus* (or *Parasynechococcus*, (Coutinho et al., 2016) and high and low nucleic acid bacteria (HNA and LNA, respectively) were enumerated every 2 h at Plymouth Marine Laboratory using flow cytometry (Tarran et al., 2006). Surface ocean concentrations of chlorophyll *a* (on GF/F) were determined on every sample

375 (Welschmeyer, 1994). Concentrations of dissolved cobalt were measured in separate samples collected from 40 m from 4 stations only using high resolution inductively coupled plasma mass spectrometry (HR-ICP-MS), preceded by UV-digestion and off-line preconcentration into a chelating resin (WAKO) at the University of Southampton (Lough et al., 2019; Rapp et al., 2017).

### 380 2.3 Global metaproteomic analysis

At 7 stations, McLane pumps were deployed to 15 m (see Table S1 for deployment details). Data from station 1 was omitted from this study due to significant riverine influence (Kunde et al., 2019). Pumps were fitted with a trace metal clean mini-MULVS filter head. Between 17 and 359 L of seawater was filtered through a 51 µm (Nitex), 3 µm (Versapor) and 0.2 µm (Supor) filter stack. Filters were immediately frozen at -80°C, with 385 subsequent transportation and storage at -80°C. Protein biomarker analysis was conducted on the 0.2 µm filter, representing the 0.2 to 3 µm particle fraction. Briefly, upon return to the laboratory, the total microbial protein was extracted using a detergent based method. The filter was unfolded and placed in an ethanol rinsed tube, then

**Deleted:** Sampling

**Deleted:** was performed

**Deleted:** )

**Deleted:** along a zonal transect between Guadeloupe and Tenerife at approx. ~22°N between 26<sup>th</sup> June and 12<sup>th</sup> August 2017 (

covered in 1 % SDS extraction buffer (1 % SDS, 0.1M Tris HCl pH 7.5, 10 mM EDTA), incubated at room temperature for 10 mins, then at 95 °C for 10 mins, and then shaken at room temperature for 1 h. The extract was 395 decanted and clarified by centrifugation before being concentrated by 5 kD membrane centrifugation to a small volume, washed in extraction buffer, and concentrated again. The total protein concentration was determined by BCA assay (kit) at this time. The proteins were precipitated in cold 50 % methanol 50 % acetone 0.5 mM HCl at 20 °C for one week, collected by centrifugation at 4 °C, and dried by vacuum. Purified protein pellets were resuspended in 1% SDS extraction buffer and redissolved for 1 h at room temperature. Total protein was again 400 quantified by BCA assay to assess recovery of the purification.

Extracted proteins were immobilized in a small volume polyacrylamide tube gel using a previously published method (Lu and Zhu, 2005; Saito et al., 2014). LC-MS/MS grade reagents were used and all tubes were ethanol rinsed. The gels were fixed in 50 % ethanol, 10 % acetic acid, then cut into 1mm cubes and washed in 50:50 acetonitrile: 25 mM ammonium bicarbonate for 1 h at room temperature, then washed again in the same 405 solution overnight. Next, the gels were dehydrated by acetonitrile treatment before protein reduction by 10 mM dithiothreitol treatment at 56 °C for 1 h with shaking. Gel pieces were rinsed in 50:50 acetonitrile: ammonium bicarbonate solution, then proteins were alkylated by treatment with 55 mM iodacetamide at room temperature for 1 h with shaking. Gels were again dehydrated by acetonitrile treatment and dried by vacuum. Finally, proteins 410 were digested by treatment with trypsin gold (Promega) prepared in 25 mM ammonium bicarbonate at the ratio of 1:20 µg trypsin: ug total protein overnight at 37 °C with shaking. The next morning, any supernatant was decanted into a clean microfuge tube, and 50 µL protein extraction buffer (50 % acetonitrile, 5 % formic acid in water) was added to the gels, incubated for 20 mins, centrifuged and collected. The extraction was repeated and combined with the original supernatant. Peptides were concentrated to approximately 1 µg total protein per µL solution by vacuum at room temperature. 10 µL or 10 µg were injected per analysis.

415 Global metaproteome analysis, which is conducted with no prior determined targets, was performed in Data-Dependent-Acquisition (DDA) mode using Reverse Phase Liquid Chromatography – active modulation – Reverse Phase Liquid Chromatography Mass Spectrometry (RPLC-am-RPLC-MS) (McIlvin and Saito, 2021). RPLC-am-RPLC-MS involves two orthogonal chromatography steps, which are performed in-line on a Thermo Dionex Ultimate 3000 LC system equipped with two pumps. The first separation was on a PLRP-S column 420 (200 µm × 150 mm, 3 µm bead size, 300 Å pore size, NanoLCMS Solutions) using an 8 h pH 10 gradient (10 mM ammonium formate and 10 mM ammonium formate in 90% acetonitrile), with trapping and elution every 30 mins onto the second column. The second separation occurred in 30 min intervals on a C18 column (100 m × 150 mm, 3 µm particle size, 120 Å pore size, C18 ReproSil-God, Maisch, packed in a New Objective PicoFrit column) using 0.1% formic acid and a 0.1% formic acid in 99.9% acetonitrile. The eluent was analyzed 425 on a Thermo Orbitrap Fusion mass spectrometer with a Thermo Flex ion source. MS1 scans were monitored between  $m/z$  380 and 1,580, with an  $m/z$  1.6 MS2 isolation window (CID mode), 50 ms maximum injection time and 5 s dynamic exclusion time.

430 Resulting spectra were searched in Proteome Discoverer 2.2 with SequestHT using a custom DNA sequence database consisting of over 30 genomes from cyanobacteria isolates and metagenomic data from the Pacific and Atlantic oceans (including metagenomes from Metzyme and Geotraces cruise GA03). Annotations were derived using BLASTp against the NCBI non-redundant protein database. The corresponding protein

**Deleted:** m

FASTA file is available with the raw mass spectra files (see Supplement A). SequestHT parameters were set to +/1 10 ppm for the parent ion, 0.6 Da for the fragment, with cysteine modification (+57.022) and variable methionine (+16.0) and cysteine oxidation allowed. Protein identifications were made using Protein Prophet in Scaffold (Proteome Software) at the 95 % peptide confidence level, resulting in <1 % protein and peptide FDRs. Details of the peptides identified relative to protein name and organism can be found in Table S2 and the protein report and analytical details can be found in Supplement B.

[Global metaproteome protein abundances are reported in normalized spectral counts. The normalization](#)

435 [is performed by summing the total number of spectra in each sample, calculating the average number of spectra across all the samples, and then multiplying each spectrum count by the average count over the sample's total spectral count. This is done to control for small differences in the amount of sample injected into the mass spectrometer.](#)

**Formatted:** Font: (Default) Times New Roman

**Formatted:** Indent: First line: 1.27 cm, Line spacing: 1.5 lines

#### 440 2.4 Quantitative proteomics analysis

A small number of tryptic peptides were selected for absolute quantitative analysis in the samples from nutrient addition experiments (see section 2.5 for details) and were analysed as described [in detail](#) by Held et al., 2025 (companion manuscript). The amino acid sequence for the protein biomarkers quantified in this study (PstS, PhoA, PhoX) for *Prochlorococcus* and *Synechococcus* are summarised in Table S3 and peptide report and

445 analytical details are found in Supplement C.

**Deleted:** (submitted)

#### 2.5 Nutrient bioassay experiments

Trace-metal clean sampling and incubation protocols used to setup onboard bioassays are described in detail in the Supplement D. Aliquots of Fe, Zn and Co solutions were added to unfiltered seawater to investigate metal 450 limitation of alkaline phosphatase and results are reported in Held et al., (submitted). Alongside these experiments, we added DOP alone or with Fe and Zn to investigate the potential for organic P availability to influence AP activity at stations 2 and 3 only, where concentrations of DOP were low (< 80 nM, Fig. 1a and e, Table S4), and the results are reported here. Trace-metal clean 20L carboys were triple rinsed with unfiltered seawater collected from 40m (to avoid contamination from the ship) via the FISH and filled and amended

455 accordingly (Table S4). [At the start and end of 48 hours, we measured phytoplankton biomass \(chlorophyll a, abundance of \*Prochlorococcus\*, \*Synechococcus\*\) and AP activity. After 48 hours, we collected samples to quantify protein concentration](#) (PstS, PhoA and PhoX) as described in section 2.4 (Table S3). Incubations were conducted in triplicate. However, due to the biomass (therefore volume) required for protein analysis, we were unable to collect samples from three incubation bottles for further analyses. Instead, all measurements were

**Deleted:** W

**Deleted:** the change in

**Deleted:** at the start of the incubations and after 48 h

**Deleted:** W

**Deleted:** also

**Deleted:** quantified the concentration of proteins

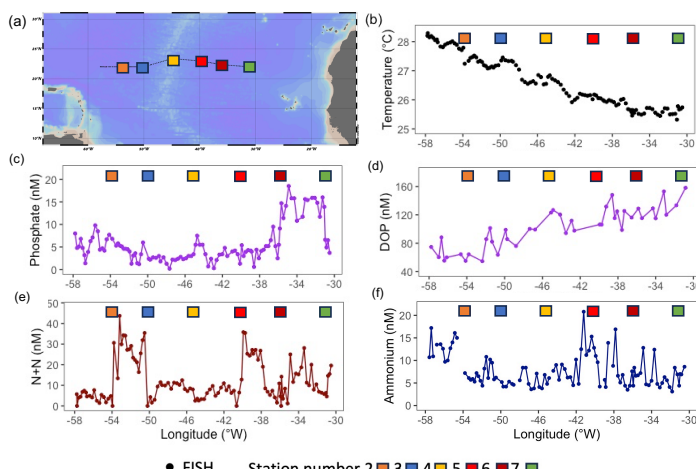
455 collected from two incubation bottles, except aliquots for determination of AP, which was collected from three incubation bottles. To compare the change in states or rates in treatments relative to the control, we considered a significant change in a property to occur when the mean of the property in the amended incubation was 2-times higher (or lower) than the mean control incubation. Incubations were conducted in a temperature controlled container set to a temperature measured at 40m (between 25 and 27°C) and with 12:12h light:dark cycle

460 470 simulated by LED light panels (Part no: LED-PANEL-300-1200-DW and LED-PANEL-200-6-DW, Daylight White, supplier Power Pax UK Limited).

### 3. Results and Discussion

#### 3.1. Zonal trends in nutrients, cell abundance and biological rates:

485 Strong zonal gradients were evident in surface temperature and phosphorus concentrations. From west to east, SST decreased by ~ 3 °C (Fig. 1b), phosphate increased by ~ 15 nM (Fig. 1c) and DOP increased 3-fold (from ~ 50 nM to ~ 150 nM, Fig. 1d). By comparison, there were no clear zonal trends in fixed nitrogen, with concentrations of nitrate plus nitrite (N+N, herein nitrate) ranging from < 10 nM to ~ 40 nM (Fig. 1e) and ammonium, which ranged from 3 to 21 nM, being highest at stations 5 and 6 (Fig. 1f).



495 Figure 1. (a) Locations sampled during JC150 from the trace metal clean towed FISH (black circles) and stations (coloured squares) and surface ocean properties including (b) sea surface temperature (°C), (c) phosphate (nM), (d) dissolved organic phosphorus (DOP, nM), (e) nitrate+nitrite (N+N, nM), (f) ammonium (nM). Note that data from JC150 Station 1 (test station) has not been included in this manuscript due to the strong riverine influence (Kunde et al., 2019). Map produced using Ocean Data View (ODV).

500 There was a clear zonal trend in dissolved Fe concentrations, which decreased west to east by ~ 1.0 nM (Fig. 2a) owing to enhanced Saharan dust deposition in the western Atlantic Ocean (Kunde et al., 2019). In contrast, Zn concentrations were variable throughout the transect (ranging from 0.04 to 0.8 nM, Fig. 2b) and cobalt was constant (~ 11 pM to 14 pM, data not shown).

505 Microbial biomass, picocyanobacteria abundance and biological rates exhibited strong zonal gradients. From west to east, there were increases in chlorophyll *a* concentration (Fig. 3a) and *Prochlorococcus* cell abundance (Fig. 3b) whereas *Synechococcus* cell abundance decreased (Fig. 3c). HNA and LNA bacterial abundance (Fig.

**Deleted:** 1

**Deleted:** states

**Formatted:** Line spacing: 1.5 lines

**Deleted:** SST decreased from ~ 28 °C in the west to ~ 25 °C in the east (Fig. 1b). In the upper 10 m, phosphate increased from ~ 5 nM to 20 nM from west to east (Fig. 1c), whereas nitrate plus nitrite (N+N, herein nitrate) ranged from < 10 nM to ~ 40 nM with no clear zonal trend (Fig. 1d). Ammonium concentrations ranged from 3 to 21 nM, with the highest concentrations observed between stations 5 and 6 (Fig. 1f). From west to east, DOP increased 3-fold (from ~ 50 nM to ~ 150 nM, Fig. 1e) alongside a 4-fold decrease in chlorophyll corrected AP activity (from > 2000 nmol P µg chl *a* d<sup>-1</sup> to < 500 nmol P µg chl *a* d<sup>-1</sup>, Fig. 1g). Concurrent zonal gradients of phosphate, DOP and AP activity supports previous findings (Mahaffey et al., 2014) of an increase in AP activity as phosphate decreases (Fig. S1a), driving a decline in DOP (Fig. S1b). 1

**Deleted:** nitrate+nitrite (N+N, nM),

**Deleted:** dissolved organic phosphorus (DOP, nM),

**Deleted:**,

**Deleted:** (g) chlorophyll *a* – corrected rates of alkaline phosphatase (nmol P mg chl d<sup>-1</sup>), (h) mean rates of dinitrogen (N<sub>2</sub>) fixation (nM N d<sup>-1</sup>) with error bars as standard deviation of triplicate incubations.

**Deleted:** Dissolved Fe concentrations decreased from ~ 1.4 nM in the west to ~ 0.4 nM in the east (Fig. 2a), with higher Fe in the west due to enhanced dust deposition from the Saharan dust source that is transported to the western Atlantic Ocean (Kunde et al., 2019). Zn was variable throughout the transect, ranging from 0.04 to 0.8 nM (Fig. 2b). Cobalt was measured at 40 m and at 4 stations only and ranged from 11 pM at stations 2 and 3 to 13–13.9 pM at stations 4 and 7 (data not shown).

**Formatted:** Line spacing: 1.5 lines

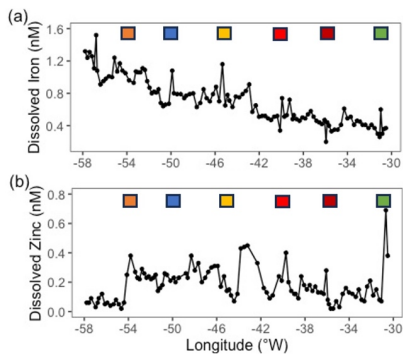
**Commented [NH4]:** could we drop this into a supplemental table or is someone planning to write a paper about this?

**Formatted:** Font: (Default) Times New Roman

3d and e, respectively) also increased from east to west. There was also a 4-fold decrease in chlorophyll corrected APA (from  $> 2000 \text{ nmol P } \mu\text{g chl } a \text{ d}^{-1}$  to  $< 500 \text{ nmol P } \mu\text{g chl } a \text{ d}^{-1}$ , Fig. 3f), likely in response to the observed gradient in P/DOP availability (Mahaffey et al., 2014, Fig. S1a, S1b).

540 In addition, the abundance of key diazotrophs *Trichodesmium* and UCYN-A increased from west to east (Cerdan-  
Garcia et al., 2022). Although rates of  $\text{N}_2$  fixation in the east exceeded those in the west (3 to 10 nM d<sup>-1</sup> and < 3  
nM d<sup>-1</sup>, respectively), the highest rates were in the central transect between stations 4 and 5 (12 to 18 nM d<sup>-1</sup>, Fig.  
3g).

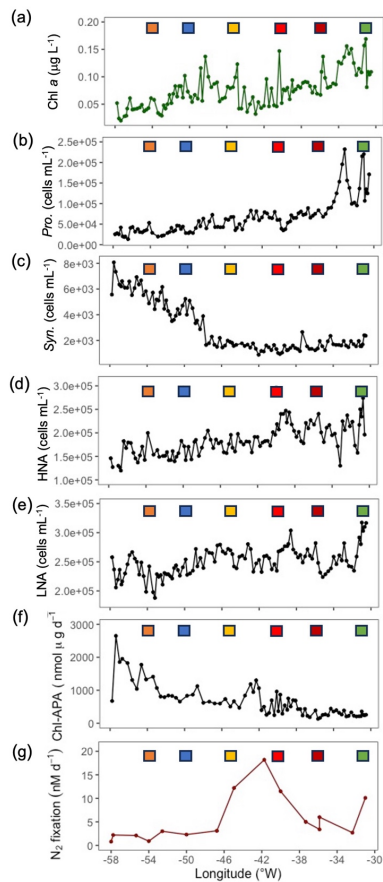
Formatted: Line spacing: 1.5 lines



545 Figure 2. Zonal gradients in (a) dissolved iron concentrations (nM, from Kunde et al., 2019) and (b) dissolved zinc concentrations (nM). Samples captured from the towed FISH at ~ 7m. Coloured square represent stations sampled during JC150 (see Fig. 1 for station names).

550

**Deleted:** Chlorophyll *a* concentration increased from ~ 0.05  $\mu\text{g L}^{-1}$  to ~ 0.15  $\mu\text{g L}^{-1}$  from west to east (Fig. 3a). *Prochlorococcus* cell abundance increased from ~  $5 \times 10^4 \text{ cells mL}^{-1}$  in the west to  $2.5 \times 10^5 \text{ cells mL}^{-1}$  in the east (Fig. 3b), whereas *Synechococcus* cell abundance decreased from ~  $8 \times 10^3 \text{ cells mL}^{-1}$  in the west to  $1 \times 10^3 \text{ cells mL}^{-1}$  (Fig. 3c). Both HNA and LNA bacterial abundance increased ~ 2-fold from west to east (Fig. 3d and e, respectively). Rates of  $\text{N}_2$  fixation were highest between stations 4 and 5 (12 to 18 nM d<sup>-1</sup>) and were elevated in the east (3 to 10 nM d<sup>-1</sup>) compared to the west (< 3 nM d<sup>-1</sup>) (Fig. 1g). In addition, there was an increase in the abundance of key diazotrophs *Trichodesmium* and UCYN-A in the east relative to the west (Cerdan-Garcia et al., 2021).



565 Figure 3. Zonal gradients in (a) chlorophyll a concentrations ( $\mu\text{g chl L}^{-1}$ ) and the abundance of (b)  
 566 *Prochlorococcus* (cells  $\text{mL}^{-1}$ ), (c) *Synechococcus* (cells  $\text{mL}^{-1}$ ), (d) high nucleic acid bacteria (HNA, cells  $\text{mL}^{-1}$ )  
 567 and (e) low nucleic acid bacteria (LNA, cells  $\text{mL}^{-1}$ ), (f) chlorophyll a – corrected rates of alkaline phosphatase  
 568 ( $\text{nmol P mg chl d}^{-1}$ ) and (g) mean rates of dinitrogen ( $\text{N}_2$ ) fixation ( $\text{nM N d}^{-1}$ ) with error bars as standard  
 569 deviation of triplicate incubations. Samples captured from the towed FISH at  $\sim 7\text{m}$ . Coloured squares represent  
 570 stations sampled during JC150 (see Fig. 1 for station names).

**Deleted:** .

These zonal gradients in hydrography, nutrients, biological rates and picocyanobacteria create two contrasting regions – one in the west (west of  $46^{\circ}\text{W}$  or west of station 4) and one in the east (east of  $46^{\circ}\text{W}$  or east of station 4). Thus, quantitative comparisons of key characteristics can be drawn between Station 2 at  $54^{\circ}\text{W}$  and Station 7 at  $31^{\circ}\text{E}$  (Fig. 1a, Table 2). Compared to the east, conditions in the west were characterized by notably

**Deleted:** .

**Formatted:** Indent: First line: 1.27 cm, Line spacing: 1.5 lines

higher dissolved Fe and ammonium concentrations (3 to 4-fold higher), APA (4-fold higher) and *Synechococcus* abundance (2-fold higher). In contrast, the east was characterized by relatively high phosphate, DOP, chlorophyll *a*, *Prochlorococcus* abundance, rates of N<sub>2</sub> fixation, *Trichodesmium* and UCYN-A abundances (Table 2).

Based on these biogeochemical parameters, the phosphate-binding protein PstS, which is expressed under P-limiting conditions, would be expected to be prevalent throughout the transect consistent with low phosphate concentrations across the entire transect. Protein biomarkers would also be expected to indicate higher alkaline phosphatase (AP) abundances in the west, corresponding with the observed trends in APA. In addition, PhoX would be expected to be prevalent in the Fe-rich west, with greater prevalence of Fe-stress biomarkers in the east.

Properties higher in the west (-fold)	Properties higher in the east (-fold)
Iron (3) *	Phosphate (4) *
Ammonium (4) *	DOP (3) *
APA (4) *	Chlorophyll (2) *
V <sub>max</sub> /K <sub>m</sub> (5) <sup>1</sup>	<i>Prochlorococcus</i> (6) *
<i>Synechococcus</i> (2) *	N <sub>2</sub> fixation rates (3) **
<i>Prochlorococcus</i> -Phosphate binding protein, PstS (2) <sup>1</sup>	<i>Trichodesmium</i> (2) <sup>1</sup>
<i>Prochlorococcus</i> -alkaline phosphatase, PhoA (7) <sup>1</sup>	UCYN-A (71) <sup>1</sup>
<i>Synechococcus</i> -alkaline phosphatase, PhoA (29) <sup>1</sup>	<i>Prochlorococcus</i> - Nitrogen regulatory protein, PII (1.3) <sup>1</sup>
SAR11-alkaline phosphatase, PhoA (24) <sup>1</sup>	<i>Prochlorococcus</i> - Ammonium transporter, AmtB (1.7) <sup>1</sup>
Total <i>Synechococcus</i> protein (1.3) <sup>1</sup>	<i>Prochlorococcus</i> -Urea permease, UrtA (1.6) <sup>1</sup>
	<i>Prochlorococcus</i> -Ferredoxin (9) <sup>1</sup>
	<i>Prochlorococcus</i> -Zinc peptidase (1.3) <sup>1</sup>
	<i>Prochlorococcus</i> -Zinc transporter (4) <sup>1</sup>
	<i>Prochlorococcus</i> - Cobalamin synthetase (5) <sup>1</sup>
	SAR11- alkaline phosphatase, PhoX (4) <sup>11</sup>
	Total <i>Prochlorococcus</i> protein (1.6) <sup>1</sup>

Table 2. Summary of states, rates and protein biomarkers that are higher in the west (left hand column) or east (right hand column) of the transect. The numbers in brackets represent the approximate -fold difference between west and east. Properties not reported (e.g. dissolved zinc, *Syn-UrtA*) displayed no clear difference between west and east. We note if the differences in properties are statistically significant (\*, p < 0.05) or not significant (\*\*, p > 0.05). <sup>1</sup> indicates insufficient replication or measurements for statistical analysis.

### 3.2 Zonal gradients in phosphorus acquisition proteins

#### 3.2.1. *Prochlorococcus*

Zonal gradients in *Prochlorococcus* P proteins generally indicate more severe P stress in the west.

*Prochlorococcus* (HLII) specific P proteins PstS and PhoA (*Pro*-PstS and *Pro*-PhoA, respectively) were almost 2-fold and 7-fold higher in the west relative to the east (Fig. 4a, Table 2), whereas there was no clear zonal trend in PhoX (*Pro*-PhoX, Fig. 4a). Similar zonal trends for PstS (Fig. S2a), PhoA (Fig. S2b) and PhoX (Fig. S2c) were observed irrelevant of the strain or ecotype of *Prochlorococcus*, thus reflecting true biological regulation within the entire *Prochlorococcus* community, rather being contingent on variation in the abundance of one clade/strain across the transect. Moreover, the increase in total *Prochlorococcus* protein (Fig. 4d) alongside *Prochlorococcus* cell abundance (Fig. 3b) in the east suggests that trends in untargeted metaproteomics analysis

**Deleted:** The zonal gradients in the hydrography, nutrients, biological rates and cyanobacteria create two contrasting regions in the west (west of 46°W or west of station 4) and east (east of 46°W or east of station 4), allowing a quantitative comparison of key characteristics between station 2 at 54°W and station 7 at 31°E (Fig. 1a, Table 2). In the west, concentrations of dissolved Fe and ammonium, averaged over mixed layer, were 3 to 4-fold higher, APA was 4-fold higher and *Synechococcus* abundance was 2-fold higher compared to the east. In contrast in the east, phosphate, DOP and chlorophyll *a* were 2 to 4-fold higher, *Prochlorococcus* abundance was 6-fold higher, rates of N<sub>2</sub> fixation were 3-fold higher (excluding maximum rates at stations 4 and 5) and *Trichodesmium* and UCYN-A abundances were 2 and 71-fold higher (Table 2).

**Deleted:** With low phosphate concentrations across the entire transect,

**Formatted:** Indent: First line: 1.27 cm, Line spacing: 1.5 lines

**Deleted:** Against a background of low phosphate concentrations along the entire transect, we would expect PstS to be prevalent throughout the basin, indicating phosphate stress. At the same time, we would expect a strong west-east gradient in protein biomarkers indicative of higher AP in the west to match the observed trends in rates of APA. We would expect prevalence of PhoX in this Fe-rich basin and Fe-stress biomarkers to be more prevalent in the east where dissolved Fe concentrations were lower. <sup>11</sup>

**Formatted:** Superscript

**Formatted:** Superscript

**Formatted:** Superscript

**Formatted:** Superscript

**Deleted:** west

**Formatted:** Superscript

**Formatted:** English (US)

**Deleted:** Phosphorus acquisition by

**Formatted:** Line spacing: 1.5 lines

**Deleted:** For *Pro*-PstS and *Pro*-PhoA, the zonal trends were consistent across other clades of *Prochlorococcus* for PstS (Fig. S2a), PhoA (Fig. S2b) and PhoX (Fig. S2c).

**Formatted:** Font: Not Italic

are representative of microbial community structure. Thus, assuming all observed *Prochlorococcus* cells possess both genes, the higher *Pro-PstS* and *Pro-PhoA* in the west, where *Prochlorococcus* abundance was lower, reflects a physiological response to low phosphorus availability.

**Deleted:** Note that total *Prochlorococcus* protein (reported as total spectral counts, Fig. 4d) agreed with the zonal trend *Prochlorococcus* cell abundance (Fig. 3b) suggesting that untargeted metaproteomics analysis can capture trends in microbial community structure. Thus, higher *Pro-PstS* and *Pro-PhoA* in the west where there was lower *Prochlorococcus* reflects a physiological response to the nutrient environment rather than reflecting changes in biomass.

**Deleted:** likely

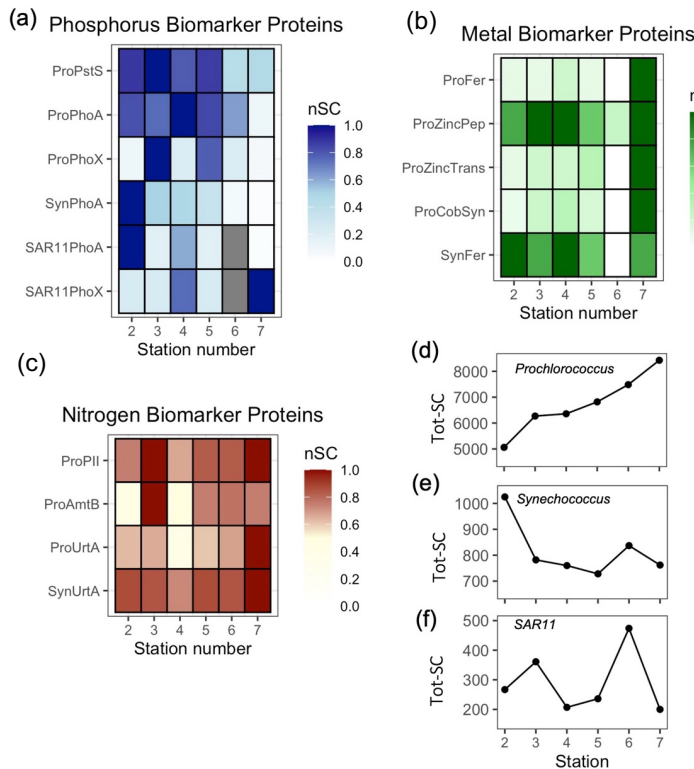
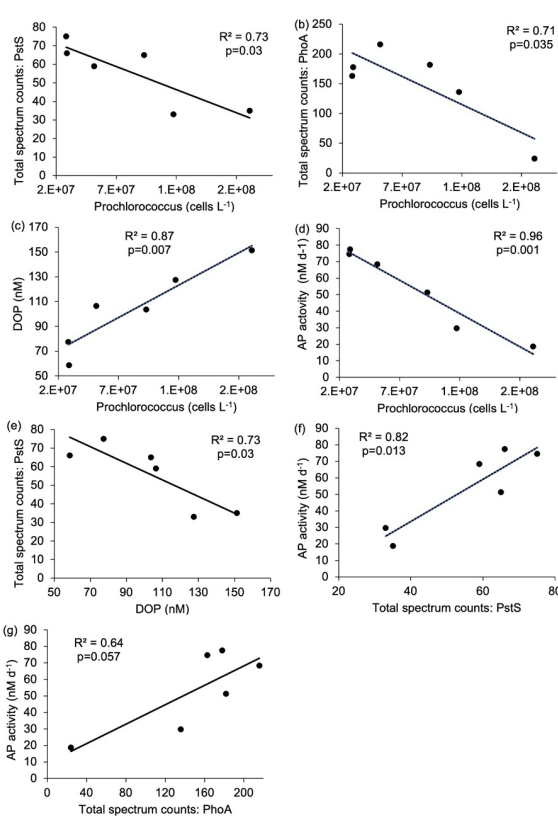


Figure 4. Zonal gradients in the spectral counts (SC) of biomarker proteins in *Prochlorococcus* (Pro-), *Synechococcus* (Syn-) and SAR11 for (a) Phosphorus biomarker proteins; PstS, PhoA and PhoX, (b) Iron, zinc and cobalt biomarker proteins; Ferredoxin (Fd) and Zinc peptidase (ZincPep), Zinc transporters (ZincTrans) and Cobalamin Synthetase (CobW) (c) Nitrogen biomarker proteins: PII, AmtB and UrtA and (d) total protein for *Prochlorococcus*, (e) *Synechococcus* and (f) SAR11, presenting an independent measure of biomass. See Table 1 for details of the protein functions. nSC represents normalized spectral counts, which represents the spectral counts normalized to the maximum value of each protein across 6 stations. Tot-SC represents the sum of all normalized spectral counts for *Prochlorococcus*, *Synechococcus* or SAR11

Correlations between *Prochlorococcus* abundance and other measured parameters also indicate a physiological response to nutrient availability. *Prochlorococcus* cell abundance was negatively correlated with *Pro-PstS* (Fig. 5a), *Pro-PhoA* (Fig. 5b) and APA (Fig. 5d). APA was also positively correlated with *Pro-PstS* and *Pro-PhoA* (Fig. 5f and g). Conversely, DOP concentration was positively correlated with *Prochlorococcus* cell abundance (Fig. 5c) but negatively correlated with *Pro-PstS* (Fig. 5e). Together these data suggest *Prochlorococcus* in the west were more P stressed than those in the east.

**Formatted:** Line spacing: 1.5 lines



**Deleted:** *Prochlorococcus* cell abundance (and in turn, total *Prochlorococcus* protein) was negatively correlated with *Pro-PstS* ( $p=0.03$ , Fig. 5a), *Pro-PhoA* ( $p=0.035$ , Fig. 5b) and APA ( $p=0.001$ , Fig. 5d) and positively correlated with DOP ( $p=0.007$ , Fig. 5c). *Pro-PstS* was negatively correlated with DOP ( $p=0.03$ , Fig. 5e) and both *Pro-PstS* and *Pro-PhoA* were positively correlated with AP activity ( $p=0.013$  and  $p=0.057$ , respectively, Fig. 5f and g). In agreement with biogeochemical signatures for P stress, proteins, *Pro-PstS* and *Pro-PhoA* were more prevalent in the west (Fig. 4a, Table 2) and significantly positively correlated to AP activity (Fig. 5f and g). However, *Prochlorococcus* abundance was lower in the west compared to the east (Fig. 3b), and negatively related to overall AP activity, *Pro-PstS* and *Pro-PhoA* and positively related to DOP concentrations. Together these data imply increased P stress of *Prochlorococcus* in the west compared to the east. This was again evident in greatly increased P-stress biomarkers in the west, despite decreasing *Prochlorococcus* abundance, demonstrating the change in biomarkers is not simply due to changing biomass.

670

Figure 5. Relationship between (a) *Prochlorococcus* cell abundance (cells L<sup>-1</sup>) and Pro-PstS (total spectrum counts), (b) *Prochlorococcus* cell abundance (cells L<sup>-1</sup>) and Pro-PhoA (total spectrum counts), (c) *Prochlorococcus* cell abundance (cells L<sup>-1</sup>) and dissolved organic phosphorus (DOP, nM), (d) *Prochlorococcus* cell abundance (cells L<sup>-1</sup>) and rates of alkaline phosphatase (APA, nM d<sup>-1</sup>), (e) DOP and Pro-PstS, (f) Pro-PstS and APA and (g) Pro-PhoA and APA. Results are linear regression as reported as R<sup>2</sup> value and p-value. Relationships shown in (a) to (f) are considered statistically significant as p < 0.05.

675 The bioassay experiments shed further light on the nutrient status of these communities. At Station 2, mean chlorophyll a increased (from 0.075 to 0.120  $\mu$ g L<sup>-1</sup>) after the addition of DOP alone, but with no increase in APA. Instead, DOP+Fe stimulated an increase in chlorophyll  $\mu$  (from 0.075 to 0.108  $\mu$ g L<sup>-1</sup>) alongside an increase in mean APA (3.03 to 9.70 nM d<sup>-1</sup>, \* denotes a 2-fold or greater increase relative to the control in Fig. 6a, Table S5). *Pro-PhoX* concentration more than doubled following DOP and, separately, DOP+Zn addition at Station 2 (Fig. 6a), however insufficient understanding of the controls on PhoX limits interpretation of this 680 observation at this time. By comparison, no significant changes in chlorophyll a or APA were observed at Station 3 (Fig. 6b, Table S5).

685 Formatted: Font: Italic

In the bioassays, DOP addition resulted in a decrease in the concentration of *Pro-PstS* and *Pro-PhoA* after the (Fig. 6a and b), implying P acquisition proteins are repressed in the presence of elevated DOP. These observations corroborate in-situ observations as *Pro-PstS* and *Pro-PhoA* both decreased to the east (Fig. 4a) where DOP and phosphate were elevated in surface waters (Fig. 1c and e). We interpret this DOP effect to be the result of DOP conversion to phosphate by alkaline phosphatase, and negative regulation of the Pho operon that controls both *PstS* and *PhoA* rather than DOP directly interacting with the regulatory system (Martiny et al., 2006). Alternatively, there may be another system that is directly regulated by DOP availability. For example, *PtrA* is an alternative phosphate-sensitive regulator identified in some *Synechococcus* and *Prochlorococcus* strains and that may be responsive to organic P (Ostrowski et al., 2010). However, flow cytometry-derived *Prochlorococcus* abundance declined in all experiments (Fig. 6a and b, Table S5), a common outcome for marine oligotrophs in bottle incubation experiments, and it is unclear whether the observed decline in *Pro-PstS* and *Pro-PhoA* in the bioassays was due to a physiological response to elevated DOP or a decline in *Prochlorococcus* biomass, or a combination of the two.

That said, knowledge of the dominant *Prochlorococcus* clades in the Atlantic Ocean (Johnson et al., 2006) alongside selection of protein markers to target specific clades allows us to interpret ecotype-level responses in experiments and in the biogeochemical transect (Saito et al., 2015). For example, *Prochlorococcus* HLII, the dominant clade in the oligotrophic subtropical ocean, can use ATP but no other organic P sources and minimally increases APA in response to P starvation as it lacks regulatory genes that respond to P-limitation (e.g. *ptrA*, Moore et al., 2005). By contrast, HL1 (MED4), which possesses both regulatory genes involved in phosphorus metabolism, *phoBR* and *ptrA* (Martiny et al., 2006), can grow on a variety of organic P substrates and substantially increases AP activity when grown on organic P relative to phosphate (Moore et al., 2005). In the global metaproteomes, a west to east increase in *Prochlorococcus* ecotypes HL1 (Fig. S3a) and HLII (Fig. S3b) was detected, which accompanied the increases in cell abundance and total *Prochlorococcus* protein. HL1 (MED4) is more prevalent in the eastern Atlantic (Zinser et al., 2007) and in this study, we observed an increase in the contribution of HL1 to total ecotype from 6 to 8% (Fig. S3c). The eastward increase in HL1 abundance alongside its increased plasticity to grow on a variety of organic P substrates may explain why *Prochlorococcus* abundance is higher where DOP is elevated in the eastern Atlantic.

**Deleted:** Within the nutrient bioassays, there was evidence that DOP limited phytoplankton growth and activity at station 2, expressed as an increase in mean chlorophyll *a* (from 0.075 to 0.120  $\mu\text{g L}^{-1}$ ) and mean rates of APA (3.03 to 9.70 nM  $\text{d}^{-1}$ ), especially after the addition of DOP+Fe (\* denotes a 2-fold or greater increase relative to the control, Fig. 6a, see Table S5 for raw data). No significant changes to growth or activity were observed at station 3 (Fig. 6b, Table S5).

**Deleted:** there

**Deleted:** was a decline in the concentration of

**Deleted:** addition of DOP

**Deleted:** protein production is

**Deleted:** This

**Deleted:** experimental observation is supported by

**Deleted:** This

**Deleted:** was

**Deleted:** likely

**Formatted:** Font: Not Italic

**Deleted:** .

**Formatted:** Font: (Default) +Headings (Times New Roman), English (UK)

**Deleted:** means that our ability to

**Deleted:** at the ecotype level

**Deleted:** resolution both

**Formatted:** Not Highlight

**Formatted:** Not Highlight

**Formatted:** Not Highlight

**Deleted:** , as well as over large spatial transects is rapidly improving

**Formatted:** Not Highlight

**Formatted:** Font: Italic

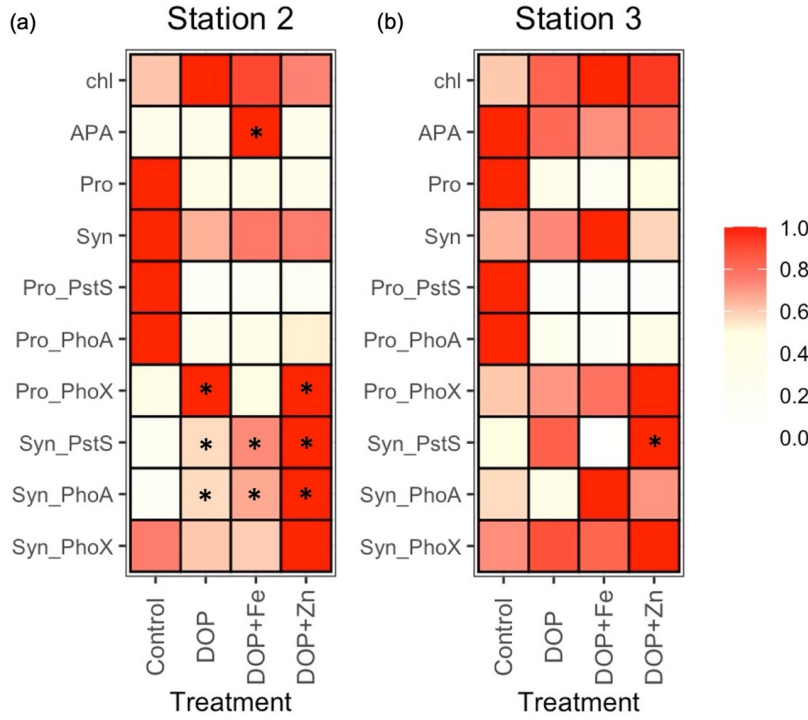
**Formatted:** Font: Italic

**Formatted:** Font: Italic

**Deleted:** 1

Through applying the global metaproteome,

**Formatted:** Font: Italic



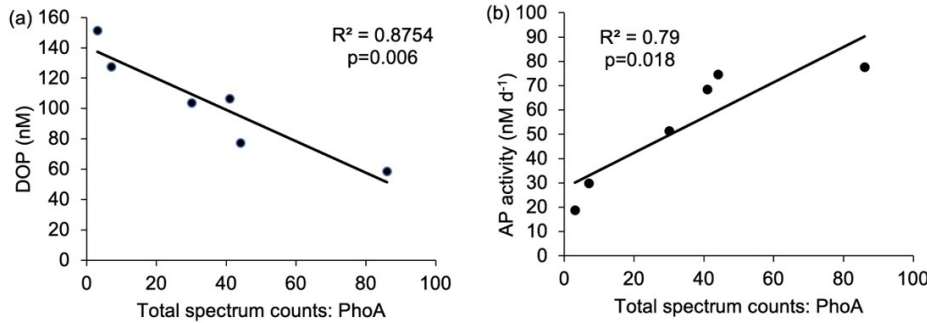
**Deleted:** (Zinser et al., 2007)(Johnson et al., 2006; Zinser et al., 2007) (Johnson et al., 2006; Zwirglmaier et al., 2007, 2008). This DOP effect was likely the result of DOP conversion to phosphate and negative regulation of the Pho operon that controls both PstS and PhoA rather than DOP directly interacting with the regulatory system. Pro-PhoX increased more than 2-fold after the addition of DOP alone and DOP+Zn at station 2 (Fig. 6a) but the lack of knowledge of controls on PhoX mean it is premature to interpret this observation. One caveat is that the abundance of *Prochlorococcus*, gleaned from flow cytometry, declined in all experiments and also eastward along the zonal transect (Fig. 6a and b, Table S5), meaning it is unclear if the decline in protein biomarkers, Pro-PstS and Pro-PhoA, in experiments and surface waters, was a physiological response to elevated DOP, or due to a decline in *Prochlorococcus* biomass. However, knowledge of the dominant *Prochlorococcus* clades in the Atlantic Ocean (Johnson et al., 2006) alongside selection of protein markers to target specific clades means that our ability to interpret at the ecotype level resolution both in experiments, as well as over large spatial transects is rapidly improving (Saito et al., 2015), highlighting the benefits of 'omics applications to study microbial biogeography.

Figure 6. Fractional (scale 0 to 1) change in states, rates and individual proteins in *Prochlorococcus* (*Pro*) and *Synechococcus* (*Syn*) after the addition of dissolved organic phosphorus (DOP), DOP and iron (DOP+Fe) and DOP and zinc (DOP+Zn) at Station 2 (a) and Station 3 (b) for chlorophyll *a* (chl), rates of alkaline phosphatase activity (APA), *Prochlorococcus* (Pro), *Synechococcus* (Syn) and protein biomarkers PstS, PhoA and PhoX. Coloured squares represent the mean of duplicate or triplicate samples and are normalised as the fraction of the maximum of that property in each experiment. See Table S4 for a description of the experiments and Table S5 for raw data for all properties. \* denotes a 2-fold or more change in the mean property relative to the control.

### 3.2.2. *Synechococcus*

PhoA in *Synechococcus* (*Syn*-PhoA) was 29-fold higher in the west than the east (Fig. 4a, Table 2) and significantly negatively correlated with DOP (Fig. 7a) and positively correlated with APA (Fig. 7b). Unlike *Prochlorococcus*, there was no correlation between cell abundance and proteins, DOP or AP (Fig. S4). The concentration of other *Synechococcus* P-related proteins (*Syn*-PstS and *Syn*-PhoX), were not detected in the sampled metaproteome but might have been present at concentrations below detection limits. In the west, *Synechococcus* abundance (Fig. 3c), APA (Fig. 1f), *Syn*-PhoA (Fig. 4a) and total *Synechococcus* protein count (Fig. 4e) were higher than in the east.

**Deleted:** 1  
**Deleted:** 3 Phosphorus acquisition by ... [6]  
**Deleted:** referred to as  
**Deleted:** compared  
**Deleted:** to  
**Deleted:** . *Syn*-PhoA was  
**Deleted:** (p=0.006,  
**Deleted:** p=0.018,  
**Deleted:** , but  
**Deleted:** u  
**Deleted:** Note that  
**Deleted:** the  
**Deleted:** ,  
**Deleted:** during  
**Deleted:** the time of sample collection and using the methods applied but may have been present albeit at low concentrations. The higher ...  
**Deleted:** in the west compared to the east coincided with higher  
**Deleted:** higher  
**Deleted:** higher  
**Deleted:** reported as total spectral counts,



825 Figure 7. Relationship between (a) *Synechococcus* PhoA (total spectral counts) and concentrations of DOP (nM) and (b) *Synechococcus* PhoA (total spectral counts) and alkaline phosphatase activity (AP, nM d<sup>-1</sup>). The R<sup>2</sup> value and p-values are reported. p<0.05 indicates that the relationship is statistically significant.

830 In the bioassays at Station 2, the addition of DOP, DOP+Fe and DOP+Zn resulted in declines in *Synechococcus* abundance by 23 to 35% relative to the control (Fig. 6a, Table S5). However, associated biomarker proteins increased. Mean concentrations of *Syn-PstS* increased by 2.7-, 3.5- and 4.7-fold after the addition of DOP, DOP+Fe and DOP+Zn, respectively, relative to the control after 48-h bioassays (Fig. 6a, Table S5). Similarly, the mean concentration of *Syn-PhoA* increased by 3.6-, 4.3- and 6.4-fold after the addition of DOP, DOP+Fe and 835 DOP+Zn, respectively (Fig. 6a, Table S5). It is unclear why production of both *Syn-PstS* and *Syn-PhoA* was more stimulated after the addition of DOP+Fe than DOP at Station 2, assuming PhoA contains Zn or Co, and not Fe as metal co-factors (Coleman, 1992). However, replication was low (n=2) and variability between replicates was high, limiting a statistically robust interpretation.

840 At Station 3, *Synechococcus* abundance increased by 12% and 53% following DOP and DOP+Fe addition, respectively but decreased after DOP+Zn addition (Fig. 6b, Table S5). The change in protein concentration after nutrient additions was less pronounced at Station 3 than Station 2 (Table S5). DOP additions induced a 1.8-fold increase in *Syn-PstS* and a 30% decrease in *Syn-PhoA*. Addition of DOP+Fe induced a 90% decrease in *Syn-PstS* and a 1.7-fold increase in *Syn-PhoA* while addition of DOP+Zn induced a 2.1-fold increase in *Syn-PstS* and a 1.2-fold increase in *Syn-PhoA* (Fig. 6b, Table S5). There was no consistent change in *Syn-PhoX* after the addition of DOP, DOP+Zn or DOP+Fe, with *Syn-PhoX* increasing or decreasing by 20 to 40% at both stations (Fig. 845 6b, Table S5).

850 In-situ measurements and bioassays converge to imply that *Synechococcus* is reliant upon organic P accessed via APA. The zonal trends and bioassay results agree with culture experiments demonstrating that *Syn-PstS* and *Syn-PhoA* are produced in the presence of DOP and Zn to increase P acquisition when phosphate is low (Cox and Saito 2013). Higher APA and prevalence of *Syn-PhoA* in the low DOP and phosphate west implies that *Synechococcus* was P stressed. Enzyme kinetic bioassays indicate higher AP enzyme efficiency in the west (Fig.

**Deleted:** The  
**Deleted:** alone  
**Deleted:** or with iron ( )  
**Deleted:** or zinc ( )  
**Deleted:** ) during 48-h bioassays caused  
**Deleted:** to decline  
**Deleted:** at station 2  
**Deleted:** at station 2, the  
**Deleted:** m  
**Deleted:** and  
**Deleted:** s  
**Deleted:** and above that of DOP alone  
**Deleted:** considering  
**Deleted:** having  
**Deleted:** so it was not possible to unpick this result statistically.  
**Deleted:** s  
**Deleted:** after  
**Deleted:** the addition of  
**Deleted:** the addition of  
**Deleted:** s  
**Deleted:** *Syn-PstS* increased by 1.8- to 2.1-fold after the addition of DOP and DOP+Zn, respectively (Fig. 6b, Table S5), whereas *Syn-PstS* decreased by 90% after the addition of DOP+Fe (Fig. 6b, Table S5). *Syn-PhoA* increased by 1.2- to 1.7-fold after the addition of DOP+Zn and DOP+Fe, respectively, but decreased by 30% after the addition of DOP only. There was no notable change in *Syn-PhoX* after the addition of DOP only, or with DOP+Zn and DOP+Fe, with *Syn-PhoX* increasing or decreasing by 20 to 40% at both stations (Fig. 6b, Table S5).  
**Deleted:** These independent results from both  
**Deleted:** i  
**Deleted:** highly dependent  
**Formatted:** Line spacing: 1.5 lines  
**Deleted:** and can produce  
**Deleted:** The capacity of *Synechococcus* to increase AP activity in the presence of organic P (Waterbury et al., 1986) and produce proteins PstS and AP under low phosphate conditions in the presence of Zn ( )  
**Deleted:** as observed in culture studies, supports our zonal trends in proteins alongside results from bioassays.  
**Deleted:** activity  
**Deleted:** occurred in a region of chronically low DOP and phosphate concentrations, implying that  
**Deleted:** Using  
**Deleted:** e  
**Deleted:** we detected

8a), with enzyme efficiency positively correlated with *Syn-PhoA* ( $p=0.017$ , Fig. 8b). Thus, *Syn-PhoA* potentially governs this trend of enzyme efficiency, suggesting DOP hydrolysis was more efficient in the west than the east.

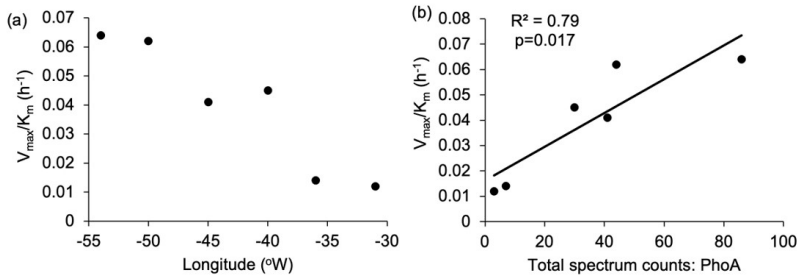


Figure 8. Enzyme efficiency for alkaline phosphatase was calculated as the ratio between  $V_{max}$  and  $K_m$  ( $\text{h}^{-1}$ ); (a) zonal gradient in enzyme efficiency, indicating higher enzyme efficiency in the western compared to the eastern subtropical Atlantic and (b) positive significant ( $p=0.017$ ) relationship between *Syn-PhoA* and enzyme efficiency.

A west-east gradient was also observed for PhoA in SAR11 (Fig. 4a), which is an abundant aerobic chemoheterotrophic alphaproteobacterial contributing to LNA bacterial counts (Fig. 3e). The abundance of both HNA and LNA (Fig. 3d and e, respectively) and total SAR11 protein (Fig. 4f) increased from west to east. However, SAR11-PhoA decreased 24-fold and SAR11-PhoX increased 4-fold (Fig. 4a, Table 2), despite dissolved Fe concentrations being higher in the west relative to the east. The mechanism for this discrepancy is unclear. However, PhoA is efficient at hydrolysing DOP under low P conditions and culture studies show that organic P is an important source of P for SAR11, representing up to 70% of its cellular P requirement when phosphate is non-limiting (Grant et al., 2019). Thus, we speculate that SAR11 might strategically use PhoA in the west with the zonal patterns in SAR11-PhoA and PhoX likely reflecting the preferential acquisition of DOP over phosphate. This further supports the premise that PhoA is an indicator of DOP acquisition across marine microbial taxa (Steck et al., 2025; Ustick et al., 2021).

The decline in *Synechococcus* abundance and *Syn-PhoA*, despite the increase in DOP in the east suggests other factors, such as resource availability or competition with other microorganisms including *Prochlorococcus*, inhibited growth of *Synechococcus* in the east. Zinc concentrations decreased eastwards from  $\sim 0.35 \text{ nM}$  to  $0.15 \text{ nM}$ . Briefly, bioassays conducted during the same expedition indicated that Zn addition stimulated a 2- to 4-fold increase in *Syn-PstS* and *Syn-PhoA* after a 48-h incubation period (Held et al., 2025; companion manuscript), corroborating a role for zinc in PhoA metabolism. Cobalt also stimulated increases in *Syn-PstS* and *Syn-PhoA*, representing new field evidence for Co influencing AP (Held et al., 2025; companion manuscript). Co may effectively substitute Zn at the active site of PhoA within marine cyanobacteria, consistent with trends observed in accelerating Co stoichiometry and APase abundances in the North Atlantic Ocean (Saito et al., 2017).

**Deleted:** which  
**Deleted:** was  
**Deleted:** We therefore speculate that  
**Deleted:** can  
**Deleted:** efficiently cleave P from natural DOP compounds even at the low DOP concentrations observed in the west.  
**Deleted:** 1

**Deleted:** We observed a similar  
**Deleted:** in  
**Deleted:** for  
**Deleted:** that contributes  
**Deleted:** While  
**Deleted:** t  
**Deleted:** increase from west to east  
**Deleted:** , also indicated by the increase in  
**Deleted:** ,  
**Deleted:** .  
**Deleted:** switch

**Deleted:** stunted  
**Deleted:** B  
**Deleted:** submitted  
**Deleted:** submitted

**Deleted:** Results from bioassays would suggest that *Syn-PhoA* should increase to the east as DOP concentration increase. Instead, we observed an eastward decline in *Synechococcus* abundance and *Syn-PhoA* alongside the increase in DOP, which suggests that other factor(s) affected the P acquisition strategy and growth of *Synechococcus*. Averaged over the upper 40m, the mean Zn concentration declined from  $\sim 0.35 \text{ nM}$  in the west to  $0.15 \text{ nM}$  in the east and may have limited *Syn-PhoA* activity. The dependence of PhoA on Zn in *Synechococcus* has been observed in culture with the production of PstS and PhoA only occurring at low phosphate as well as in the presence of Zn (Cox and Saito 2013). Held et al., (submitted) observed more than a 2- to 4-fold fold increase in *Syn-PstS* and *Syn-PhoA* after the addition of Zn or Co relative to the control, with the addition of Fe also stimulating an increase in *Syn-PstS*. This finding represents new field evidence for Co influencing AP (Held et al., (submitted), implying that Co may effectively substitute Zn at the active site of PhoA within marine cyanobacteria, consistent with trends observed in accelerating Co stoichiometry and APase abundances in the North Atlantic Ocean (Saito et al., 2017). Competition for P, trace metals and other resources with other plankton, including *Prochlorococcus* and  $\text{N}_2$  fixers, may have stunted growth of *Synechococcus* in the east relative to the western subtropical Atlantic. 1

### 3.3 Non-targeted metaproteomic indicators of nutrient status in picocyanobacteria

Higher PstS and PhoA in the west compared to the east, alongside the positive relationship between *Pro-PstS*, *Pro-PhoA* and *Syn-PhoA* with AP activity and negative relationship with DOP corroborate that these protein biomarkers are P-stress biomarkers in both *Prochlorococcus* (Martiny et al., 2006; Moore et al., 2005; Reistetter et al., 2013) and *Synechococcus* (Scanlan et al., 1993; Tetu et al., 2009). However, DOP addition stimulated distinct biomarker responses in *Prochlorococcus* and *Synechococcus* (Fig. 6, Table S5). For *Prochlorococcus*, DOP addition reduced *Pro-PstS* and *Pro-PhoA* but increased PhoX after 48 h relative to the control (Fig. 6, Table S5). In contrast, for *Synechococcus*, DOP addition increased *Syn-PstS* and *Syn-PhoA*, with no change in PhoX (Fig. 6, Table S5). We intuit that the protein biomarkers changed due to a physiological response rather than change in cell abundance because the per cell protein content (Fig. S5) showed the same pattern (with the caveat that the protein is clade specific yet likely targeted a major ecotype, whereas cell abundance represents all cells). DOP addition stimulated a decrease in *Pro-PstS* and *Pro-PhoA* per cell and increase *Pro-PhoA* per cell relative to the control (Fig. S5a), whereas DOP addition stimulated an increase in *Syn-PstS*, *Syn-PhoA* and *Syn-PhoX* per cell (Fig. S5b).

Either the protein regulatory pathway differs between *Prochlorococcus* and *Synechococcus*, and/or the strain specific differences in quantified proteins is complicating our interpretation response of proteins across different strains. Here we describe evidence for the former hypothesis. In *Prochlorococcus*, the Pho regulon controls P-acquisition genes such as *pstS* (phosphate transporter) and *phoA* and includes the two-component regulatory genes, *phoB* and *phoR* (Martiny et al., 2006). The *Pro-phoX* gene is controlled by the pho regulon as it sits within a genomic island with other P stress responsive (Kathuria and Martiny, 2011). In contrast, *Synechococcus* (WH8102) has a two-tiered phosphate response system, where the PhoBR regulator controls *pstS* using a Pho box (Cox and Saito, 2013; Tetu et al., 2009) and second regulator, *PtrA*, controls one of the *phoA* phosphatase 1000 copies, Zn transport, and various other cellular processes (Ostrowski et al., 2010). The gene neighbourhood containing *phoA* (SYNW2391) in *Synechococcus* is also located near efflux transporter and close to the ferric uptake regulator, *Fur*. To our knowledge, regulation of PhoX and its interaction with PhoA regulation in the marine picocyanobacteria is not well understood, but analysis of the gene neighbourhood in the model organism *Prochlorococcus* sp. NATL1A reveals that *phoX* is not within the *phoA* neighbourhood and is in the vicinity of a putative manganese transporter. For *Synechococcus* (WH8102), the position of *phoX* (SYN1799) is like *Prochlorococcus* and is located directly next to the *futAB* iron ABC transport system, consistent with the iron requirement of this enzyme. The separation of *phoA* and *phoX* within the genome in both *Prochlorococcus* and *Synechococcus* (at least in the representative strains described above) implies their regulation may be distinct in the different organisms. Consistent with prior observations (Browning et al., 2017; Mahaffey et al., 2014; Rouco et al., 2018), PhoA and PhoX may be regulated by both metals and phosphorus availability but the specific regulatory system in picocyanobacteria is complex and still unknown.

The alternative interpretation is that differences in strain specificity among the identified proteins explains the differences in the *Prochlorococcus* vs *Synechococcus* response patterns. Proteins concentrations are measured by

- Deleted: 6
- Deleted: P...roteomic in biomarkers as ... [7]
- Deleted: Increased prevalence of protein biomarkers
- Deleted: s
- Deleted: support previous findings that ...hese protein biomarkers are P-stress biomarkers indicators of P stress ...n both *Prochlorococcus* (Martiny et al., 2006; Moore et al., 2005; Reistetter et al., 2013) and *Synechococcus* (Scanlan et al., 1993; Tetu et al., 2009), and challenges the view that growth of picocyanobacteria are insensitive to nutrient availability. ... [8]
- Deleted: a different
- Deleted: the change in the concentration of these biomarkers after the addition of DOP in nutrient bioassays differed between *Prochlorococcus* and *Synechococcus* (Fig. 6, Table S5). For *Prochlorococcus*, DOP addition the addition of DOP ...duced the concentration of ...ro-PstS and *Pro-PhoA* but , and ... [9]
- Deleted:
- Deleted: after the 48-h incubation period relative to the control. In contrast, for
- Deleted: F...r *Synechococcus* , ... [10]
- Deleted: the addition of DOP
- Deleted: P
- Deleted: When the per cell protein content was calculated... (with the caveat that the protein is clade specific yet likely targeted a major ecotype, whereas cell abundance represents all cells) ...DOP addition stimulated a decrease in the same pattern is observed indicating that the change in protein biomarkers was not driven solely by the change in cell abundance but was rather being regulated in response to environmental conditions (Fig. S5). For *Pro-Prochlorococcus*, the ... [11]
- Deleted: decreased and
- Deleted: increased 48-h after the addition of DOP, ...relative to the control (Fig. S5a), whereas DOP addition stimulated an incr... [12]
- Formatted: Font: Italic
- Formatted: Font: Italic
- Deleted: For *Synechococcus*, the ...stS, and ... [13]
- Formatted: Font: Italic
- Formatted: Font: Italic
- Deleted: increased 48-h after the addition of DOP relative to the control, with an increase in PhoX
- Deleted: The divergence in response of the same protein biomarkers to the same substrate implies that the ... regulatory pathway for these proteins ...fers between *Prochlorococcus* and *Synechococcus*, and/or that ...he strain specific differences in quantified proteins is complicating our interpretation response of proteins across different strains. Here we describe evidence for the former hypothesis. Below, we discuss both possibilities. ... [14]
- Formatted: Adjust space between Latin and Asian text, Adjust space between Asian text and numbers
- Deleted: 1 ... [15]
- Deleted: The cellular regulation of P responsive proteins in ... [16]
- Deleted: in *Prochlorococcus* ...s controlled by the pho reg... [17]
- Formatted: Font: Italic
- Formatted
- Deleted: ... [18]
- Deleted: For *Synechococcus* (WH8102), the position of ph... [19]
- Deleted: During the nutrient bioassays, ...p ... [21]
- Deleted: were
- Deleted: quantified
- Formatted

detecting peptides, and biological specificity (e.g. to strains or species) is determined by comparing the amino acid sequence of the peptide to isolate genomes or annotated MAGs. A least-common-ancestor (LCA) analysis can then be performed to assess the level of biological specificity that is represented by that peptide (Saunders et al., 2023) (Table S3, Supplement C). The targeted peptides were selected based on their abundance in a preliminary metaproteomics analysis, suggesting that these were the most abundant proteins within the microbial community (see Held et al., 2025 for a more complete description of how targeted peptides were selected for this study region). Peptide sequences for up to 5 strains of *Prochlorococcus* were targeted with a focus on the HLII clade, particularly strain MIT9314, allowing comparison between proteins of the same strain. In contrast, protein sequences for *Synechococcus* were compared across clades because the peptide sequence for PhoA and PhoX targeted WH8102 (clade III) but the peptide sequence for PstS targeted RCC307 (clade X, Table S3). While co-occurring clades III and X are geographically positively correlated in warm oligotrophic waters (Sohm et al., 2008), RCC307 possesses a different putative alkaline phosphatase gene compared to WH8102 (likely PhoA, see Tetu et al., 2009). This mismatch in targeted strains and clades means that interpretation of the response of *Synechococcus* (and perhaps *Prochlorococcus*) to nutrient addition needs to be treated with some caution until the physiology and regulatory pathways of protein production are better understood. However, based on current knowledge of phosphate acquisition genes in marine *Synechococcus* and *Prochlorococcus*, we do expect that the targeted proteins/strains are major players in our study region.

### 3.4. Influence of trace metals on alkaline phosphatase and associated protein biomarkers

Unlike other cyanobacteria, where the trace metal availability aligns well with the biogeography of PhoA and PhoX (e.g. *Trichodesmium*, Rouco et al., 2018), there were no consistent trends between iron or zinc concentrations and proteins PhoX and PhoA respectively in this study. The distribution of Pro-PhoX from metaproteomes (Fig. 4a) did not reflect iron availability (Fig. 2a). Despite elevated iron in the west, Pro-PhoA concentrations were 2.7 to 4.7-fold higher than Pro-PhoX (reported fmol L<sup>-1</sup>, Table 3), with Pro-PhoX being greater than Pro-PhoA in the east where Fe was lowest (Fig. 2a). PhoX was not detected for *Synechococcus* in metaproteome analysis but was detected quantitatively at the start of bioassay experiments (Table 3). *Syn-PhoX* concentrations also did not reflect iron availability (Table 3) and there was no consistent trend in the ratio between *Syn-PhoA* and *Syn-PhoX* (Table 3). Zonal trends in quantitative versus metaproteome-derived *Syn-PhoA* were different and likely driven by differences in depth horizons sampled (40m for experiments, 15 meters for metaproteome analysis) as well as the different *Synechococcus* populations captured using quantitative peptide analysis (see Table S3, clade III and X) compared to metaproteomes.

Table 3: Concentration of proteins (fmol L<sup>-1</sup>) PhoX and PhoA for *Prochlorococcus* and *Synechococcus* at the start of the nutrient bioassay experiments at stations 2, 3, 4 and 7 (see Fig. 1a for locations) to illustrate how the relative concentration and ratio of PhoA to PhoX differ between *Prochlorococcus* and *Synechococcus* and across the zonal transect.

Protein biomarker	<i>Prochlorococcus</i>			<i>Synechococcus</i>		
	PhoX	PhoA	PhoA/PhoX	PhoX	PhoA	PhoA/PhoX
Protein conc. (fmol L <sup>-1</sup> )						
Station 2 control	17 ± 2	45 ± 14	2.7	21 ± 6	7 ± 1	0.3

Station 3 control	16 ± 11	48 ± 10	3.0	15 ± 2	22 ± 12	1.8
Station 4 control	7 ± 0.1	31 ± 13	4.7	9 ± 5	8 ± 3	0.8
Station 7 control	8 ± 2	3 ± 1	0.4	16 ± 2	28 ± 13	2.4

The systems biology of the PhoX enzyme is poorly understood compared to that of PstS and PhoA, where the latter is known to be regulated by phosphate and zinc (Cox and Saito, 2013; Martiny et al., 2006; Ostrowski et al., 2010; Tetu et al., 2009). Despite the lack of correlation between trace metal availability, PhoA and PhoX in the surface ocean in this study, results from bioassays conducted during the same expedition (Held et al., 2025; companion manuscript) lends support to the potential for a direct metal control on APA (Browning et al., 2017; Jakuba et al., 2008; Mahaffey et al., 2014; Saito et al., 2017). In the west, Zn addition stimulated a 6-fold increase in *Syn-PhoA* relative to the control. Cobalt addition simulated a 7-fold increase in *Syn-PhoA* and 8-fold increase in *Pro-PhoX*. Finally, iron addition stimulated a 2-fold increase in *Pro-PhoX* in the iron-deplete eastern Atlantic (Held et al., submitted). ▾

Proteins relating to iron, zinc and B<sub>12</sub> metabolism in *Prochlorococcus* increased in the east alongside the increase in *Prochlorococcus* cell abundance. Ferredoxin and zinc transporters increased eastward by 3 to 9-fold and protein annotated as CobW, a member of the COG0523 family implicated in metal chaperone functions (Edmonds et al., 2021) and Co chaperone for B<sub>12</sub> synthesis (Young et al., 2021) also increased 3 to 10-fold (Fig. 4c). The eastward increase in three independent proteins (up to 10-fold) was greater than the increase in total protein for *Prochlorococcus* (~ 1.6-fold) implying a regulated molecular increase in response to resource limitation or competition, rather than reflecting a change in biomass only. However, zinc protein annotations in *Prochlorococcus* are putative and alignment-based transporter annotations are unable to discern cognate metal use. In addition, the role of zinc in *Prochlorococcus* physiology is uncertain. *Prochlorococcus* does not have an obligate Zn requirement when phosphate is available (Saito et al., 2002), and Zn is highly toxic to a Pacific Ocean strain of *Prochlorococcus* 29/08/2025 10:57:00. In addition, while CobW is an abundant protein among the ~20 genes involved in cobalamin biosynthesis, there are currently no known biomarkers for cobalt or zinc metabolism in *Prochlorococcus*, with studies producing negative results (Hawco et al., 2020). For *Synechococcus*, there were no clear trends in ferredoxin (Fig. 4c) and flavodoxin was infrequently detected. These findings highlight the difficulty of predict the direct metal requirement alongside metals controlling multiple APs *in-situ*, and makes a strong case for continued biochemical characterization of cyanobacterial trace metal physiology and enzymes. ▾

### 3.5. Influence of nitrogen acquisition on the biogeography of *Prochlorococcus* and *Synechococcus* in the subtropical North Atlantic

We used nontargeted metaproteomics to interpret the role of nitrogen acquisition on the biogeography of *Prochlorococcus* and *Synechococcus*. Upwelling in the eastern Atlantic (Menna et al., 2015) alongside nitrogen fixation (Fig. 3g, Cerdan-Garcia et al., 2022) and dust deposition (Kunde et al., 2019) deliver fixed nitrogen including, nitrate, ammonium and urea to the surface subtropical Atlantic (dust ref here). Nitrate and ammonium concentrations were low across the transect (Fig. 1e and f), with maximum ammonium concentration coinciding

Deleted: 1

Deleted: To our knowledge the

Deleted: submitted

Formatted: Not Highlight

Formatted: Font: Italic

Formatted: Font: Italic

Formatted: Font: Italic

Deleted: Thus, further targeted experimental work is needed to determine the mechanisms

Deleted: While

Formatted: Font: Not Italic

Formatted: Font: Italic

Deleted: (Hawco and Saito, 2018)

Deleted: In conclusion, the lack of understanding of the trace metal requirement for *Prochlorococcus* and *Synechococcus*

Deleted: means it is difficult to

Formatted: Font: Italic

Moved up [2]: While the eastward increase in three independent proteins coincides with an increase in *Prochlorococcus* cell abundance and total protein spectral counts, the 4 to 9-fold increase in ferredoxin, zinc transporter and cobalamin synthetase is greater than the increase in total protein for *Prochlorococcus* (1.6-fold) implying a regulated molecular increase in response to resource limitation or competition, rather than reflecting a change in biomass only. ▾

Deleted: the eastward increase in three independent proteins coincides with an increase in *Prochlorococcus* cell abundance and total protein spectral counts, the 4 to 9-fold increase in ferredoxin, zinc transporter and cobalamin synthetase is greater than the increase in total protein for *Prochlorococcus* (1.6-fold) implying a regulated molecular increase in response to resource limitation or competition, rather than reflecting a change in biomass only. ▾

There was no consistent or significant increased phytoplankton growth, increase in *Prochlorococcus* and *Synechococcus*, or AP activity after the addition of Fe, Zn or Co alone (Held et al., submitted). However, at station 2 in the west, *Syn-PhoA* increased 6 and 7-fold after the addition of Zn (38 ± 0.56 fmol L<sup>-1</sup>) and Co (47 ± 6.8 fmol L<sup>-1</sup>) relative to the control (6.7 ± 1.5 fmol L<sup>-1</sup>), respectively. At station 4 over the mid-Atlantic ridge, *Pro-PhoX* increased 8-fold upon addition of Co relative to the control. At station 7 in the east, *Pro-PhoX* also increased over 2-fold upon Fe addition (to 18 ± 2.6 fmol L<sup>-1</sup>) relative to the control (8.2 ± 2.4 fmol L<sup>-1</sup>, Held et al., submitted). Results from these bioassays illustrate the potential for a direct metal control on AP, lending support to the hypothesis for local, albeit patchy metal-phosphorus co-limitation in the subtropical North Atlantic (Jakuba et al., 2008, Mahaffey et al., 2014, Saito et al., 2017, Browning et al., 2017). ▾

Alongside metal control of AP, there were gradients in proteins relating to iron, zinc and B<sub>12</sub> metabolism in *Prochlorococcus*. Ferredoxin increased from west (1 to 2 spectral counts) to the east (9 spectral counts) alongside zinc transporters (1 to 3 spectral counts in the west, 9 in the east) although there was no clear zonal trend in zinc peptidases (Fig. 4c, Table 2). We consider these zinc protein annotations in *Prochlorococcus* as putative because this transporter annotated in the *Prochlorococcus* genome has not been validated for Zn transport, and alignment-based transporter annotations tend to have difficulty in discerning cognate metal use. Moreover, under phosphate-replete conditions, *Prochlorococcus* does not have an obligate Zn requirement (Saito et al., 2002), and Zn is highly toxic to a Pacific Ocean strain of *Prochlorococcus* (Hawco et al., 2018), contributing to the uncertainty of the role of zinc in *Prochlorococcus*. ▾ [22]

Deleted: 5

Deleted: Controls

Deleted: on

Deleted: Untargeted

Deleted: were used to how explore

Formatted: Highlight

with the highest N<sub>2</sub> fixation rates (Fig. 3g). *Prochlorococcus* (and *Synechococcus*) are prime beneficiaries of N exuded from N<sub>2</sub> fixers (Caffin et al., 2018). *Prochlorococcus*-AmtB and UrtA was lowest where N<sub>2</sub> fixation and ammonium were highest (Figure 4b), reflecting alleviation of N stress as *Prochlorococcus* benefited from N exudates, as observed in the North Pacific gyre (Saito et al., 2014, 2015). Otherwise, eastward increases in protein biomarkers in *Prochlorococcus*, specifically P-II, ammonium transporter AmtB and urea transporter UrtA (30-70%, Fig. 4b and Table 2) indicate increasing N stress towards the eastern Atlantic for *Prochlorococcus*.

*Synechococcus* appeared to be N stressed throughout the transect as UrtA spectral counts were constant and more than 5 times higher than for *Prochlorococcus* (Fig. 4b). This is likely due to its larger cell size and less efficient surface-area to volume ratio for nutrient acquisition (Chisholm 1992). P-II and AmtB (or NtcA) was not detected in the metaproteome of *Synechococcus*, perhaps because *Synechococcus* was 5 to 10 times less abundant in the metaproteomes compared to *Prochlorococcus*. The dominance of proteins for ammonium and urea acquisition of *Synechococcus* and *Prochlorococcus* are consistent with the premise that while marine *Synechococcus* and some *Prochlorococcus* strains have the genetic makeup to assimilate nitrate (Berube et al., 2015; Domínguez-Martín et al., 2022; Martiny et al., 2009), it accounts for < 5% of their total N demand, and instead ammonium and urea are the dominant N sources (Berthelot et al., 2019; Casey et al., 2016; Painter et al., 2008)

#### 4.0. Conclusions

This study exploited natural gradients in nutrient resources created by upwelling in the east and dust deposition in the west. Combining biogeochemical states, enzyme rate measurements, and 'omics approaches, in the spirit of the developing 'BioGeoSCAPES program (Saito et al., 2024), we studied the nutrient acquisition strategies for *Prochlorococcus* and *Synechococcus* in-situ and using nutrient bioassays. Using protein biomarkers alongside biogeochemical signatures for nutrient stress, we concluded that *Prochlorococcus* and *Synechococcus* were P-stressed in the western Atlantic and *Prochlorococcus* was N-stressed in the eastern Atlantic, with *Synechococcus* showing signs of N-stress throughout the transect. Our findings are generally consistent with prior metagenomic observations on basin scale contrasts in N and P stress for *Prochlorococcus* in the Atlantic Ocean (at medium level, Ustick et al., 2021). There was evidence for trace metal control on alkaline phosphatase but the response of protein biomarkers to the addition of organic P, Zn and Fe differed between *Prochlorococcus* and *Synechococcus* (also see Held et al., 2025, companion manuscript), highlighting that the functions and systems biology of alkaline phosphatase regulation differs across the organisms and for different environmental stimuli. This indicates that ongoing laboratory characterization of protein biomarkers and cyanobacterial physiology is needed defining the regulation and function not only at the species level, but also across strains within species.

Under future climate scenarios, stratification, aerosol dynamics, N<sub>2</sub> fixation and the bioavailability of organic P are predicted to change (e.g. (Buchanan et al., 2021; Chien et al., 2016; White et al., 2012; Wrightson and Tagliabue, 2020), all with the potential to perturb the availability of already scarce nutrient resources in the oligotrophic gyres. To identify and quantify the future trajectory of *Prochlorococcus* and *Synechococcus* under future ocean scenarios, a holistic view that considers the species and strain specific strategies used to access

**Formatted:** Subscript

**Formatted:** Font: Italic

**Formatted:** Font: Italic

**Deleted:** was

**Formatted:** Font: Italic

**Formatted:** Not Highlight

**Formatted:** Font: Not Italic

**Deleted:** For *Synechococcus*, the urea transporter UrtA spectral counts were more than 5 times higher than for *Prochlorococcus* and were constant across the transect, implying *Synechococcus* was N stressed throughout the transect (Fig. 4b), likely due to its larger cell size and less efficient surface-area to volume ratio for nutrient acquisition (Chisholm 1992). We did not detect P-II and AmtB (or NtcA) in the metaproteome of *Synechococcus*, perhaps because *Synechococcus* was 5 to 10 times less abundant in the metaproteomes compared to *Prochlorococcus*. DSurface ocean nitrate (< 40 nM, Fig. 1d) and ammonium (< 20 nM, Fig. 1f) concentrations were low, with a 4-fold decrease in ammonium from west to east, and a maximum ammonium concentration coinciding with the highest rates of N<sub>2</sub> fixation (Fig. 1h). Corresponding with these chemical observations, *Prochlorococcus* protein biomarkers P-II, ammonium transporter AmtB and urea transporter UrtA increased eastward (30-70%, Fig. 4b and Table 2). We postulate that the eastward increase in these proteins, especially urea transporter UrtA (also consistent across different clades, see Fig. S2) was indicative of increasing N stress towards the eastern Atlantic in contrast to increasing P stress in the western Atlantic. The North Atlantic is a region of enhanced N<sub>2</sub> fixation owing to the supply of iron-rich dust (Moore et al 2009) and *Prochlorococcus* (and *Synechococcus*) are prime beneficiaries of N exuded from N<sub>2</sub> fixers (Caffin et al., 2018). Enhanced rates of N<sub>2</sub> fixation and higher ammonium concentrations (Figures 1h and 1f, respectively) were observed in the middle of the zonal transect (38 to 46°W, between stations 4 and 5). *Prochlorococcus*-AmtB and UrtA were lowest at these stations (Figure 4b), likely reflecting alleviation of N stress as *Prochlorococcus* benefited from N exudates, as observed in the North Pacific gyre (Saito et al 2013, Saito et al 2015). However, despite N<sub>2</sub> fixation rates being ~3-fold higher in the east compared to the west (Table 2), the overall increase in *Prochlorococcus* N stress biomarkers in the east indicates that this species may not have been the main beneficiary of this process.

**Moved up [3]:** For *Synechococcus*, the urea transporter UrtA spectral counts were more than 5 times higher than for *Prochlorococcus* and were constant across the transect, implying *Synechococcus* was N stressed throughout the transect (Fig. 4b), likely due to its larger cell size and less efficient surface-area to volume ratio for nutrient acquisition (Chisholm 1992). We did not detect P-II and AmtB (or NtcA) in the metaproteome of *Synechococcus*, perhaps because *Synechococcus* was 5 to 10 times less abundant in the metaproteomes compared to *Prochlorococcus*.

**Deleted:** In addition to N and P, where both *Prochlorococcus* and *Synechococcus* had the potential to benefit from freshly fixed N and the changes in P speciation and availability along the zonal transect, we can consider the trace element controls that could have impacted their biogeography. Upwelling in the eastern Atlantic may have delivered Fe and other trace metals to surface waters, with lateral transport potentially driving zonal gradients. However, dissolved Fe was low in the east and trace metal proteins increased relativ[...]

**Commented [MS14]:** Section reads great!

**Deleted:** In the vast subtropical ocean gyres, the abundant picoplankton species, *Prochlorococcus* and *Synechococcus*, are responsible for > 60% of primary productivity and thus are k[...]

**Deleted:** states

**Deleted:** s

**Deleted:** akin to the

**Deleted:** aspiration of the developing

**Deleted:** , with a focus on P.

**Deleted:** submitted

**Deleted:** will be useful for

resources, alongside representation of large scale forcings are required. We have shown here that there is utility in combining biochemical assays with untargeted and targeted omics approaches to reveal these patterns,

1710 generate hypotheses that can be tested in controlled laboratory experiments, and improve predictions of marine microbiology and biogeochemistry in a changing ocean.

**Competing interests:** The authors declare no competing interests

**Data availability:** All new data are provided in the Supplement or are available from the British Oceanographic Data Centre (BODC) with the following DOIs: Size-fractionated iron measurements (([Berube et al., 2015](#);

1715 [Dominguez-Martin et al., 2022](#); [Martiny et al., 2009](#))), inorganic nutrients, alkaline phosphatase, DOP, chlorophyll, flow cytometry: <https://doi.org/10.5285/284a411e-2639-93de-e063-7086abc0e9d8>), Experiment D (<https://doi.org/10.5285/1e9c4caa-b936-fc7c-e063-7086abc06ff6>). The mass spectrometry proteomics data have been deposited to the ProteomeXchange Consortium via the PRIDE partner repository with the dataset identifier PXD054252 and 10.6019/PXD054252

1720 **Supplement.** Supplementary information is provided as individual files and 1 zip file. There are 5 supplements including Supplement A (Fasta file), Supplement B (protein file), Supplement C (peptide file) and Supplement D (trace metal clean protocols for nutrient bioassays). In the zip file, there are 5 supplementary tables provided as spreadsheets (Table S1 to S5) and 5 supplementary figures (Fig. S1 to S5).

1725 **Author contributions:** CM, MCL and AT acquired the funding from NERC. CM and MCL led the research cruise. CD conducted AP measurements. KK conducted Fe measurements. NW conducted zinc measurements. MSC conducted nutrient measurements. LW conducted N<sub>2</sub> fixation measurements. CM, MCL, CD, KK, LW and NW conducted the large volume incubation experiments. KK and NH conducted the quantitative proteomics analysis and MM analysed samples using mass spectrometry at WHOI. NH and MM conducted the global metaproteome analysis. CM and NH wrote the manuscript with significant contributions from MS, ML, CD, KK and AT.

**Deleted:** L

**Deleted:** L

**Deleted:** i

1730 **Acknowledgements:** The authors would like to thank the officers and crew of the *RRS James Cook* for the successful research cruise, JC150. This research was supported by the Natural Environment Research Council (NE/N001079/1, awarded to CM and AT, NE/N001125/1 awarded to ML), Simons Foundation Grants 1038971 and BioSCOPE, Chemical Currencies of a Microbial Planet (CCOMP) NSF-STC 2019589 to M.A.S, an ETH Zurich Career Seed Grant to N.A.H, and the USCDornsife College of Arts and Sciences. K.K. was supported by 1740 Graduate School of the National Oceanography Centre Southampton (UK) the Simons Foundation (award 723552) during the writing process. The authors would also like to thank Alastair Lough and Clément Demasny for the dissolved cobalt measurements.

**Deleted:** i

## References

Barkley, A. E., Prospero, J. M., Mahowald, N., Hamilton, D. S., Popendorf, K. J., Oehlert, A. M., Pourmand, A., Gatineau, A., Panechou-Pulcherie, K., Blackwelder, P., and Gaston, C. J.: African biomass burning is a substantial source of phosphorus deposition to the Amazon, Tropical Atlantic

Ocean, and Southern Ocean, Proc. Natl. Acad. Sci., 116, 16216–16221,  
1755 https://doi.org/10.1073/pnas.1906091116, 2019.

Becker, S., Aoyama, M., Woodward, E. M. S., Bakker, K., Coverly, S., Mahaffey, C., and Tanhua, T.: GO-SHIP Repeat Hydrography Nutrient Manual: The Precise and Accurate Determination of Dissolved Inorganic Nutrients in Seawater, Using Continuous Flow Analysis Methods, *Front. Mar. Sci.*, 7, 581790, https://doi.org/10.3389/fmars.2020.581790, 2020.

Berthelot, H., Duhamel, S., L'Helguen, S., Maguer, J.-F., Wang, S., Cetinić, I., and Cassar, N.: NanoSIMS single cell analyses reveal the contrasting nitrogen sources for small phytoplankton, *ISME J.*, 13, 651–662, https://doi.org/10.1038/s41396-018-0285-8, 2019.

Berube, P. M., Biller, S. J., Kent, A. G., Berta-Thompson, J. W., Roggensack, S. E., Roache-Johnson, K. H., Ackerman, M., Moore, L. R., Meisel, J. D., Sher, D., Thompson, L. R., Campbell, L., Martiny, A. C., and Chisholm, S. W.: Physiology and evolution of nitrate acquisition in *Prochlorococcus*, *ISME J.*, 9, 1195–1207, https://doi.org/10.1038/ismej.2014.211, 2015.

Bopp, L., Resplandy, L., Orr, J. C., Doney, S. C., Dunne, J. P., Gehlen, M., Halloran, P., Heinze, C., Ilyina, T., Séférian, R., Tjiputra, J., and Vichi, M.: Multiple stressors of ocean ecosystems in the 21st century: projections with CMIP5 models, *Biogeosciences*, 10, 6225–6245, https://doi.org/10.5194/bg-1770 10-6225-2013, 2013.

Brewer, P. G. and Riley, J. P.: The automatic determination of nitrate in sea water, *Deep Sea Res. Oceanogr. Abstr.*, 12, 765–772, https://doi.org/10.1016/0011-7471(65)90797-7, 1965.

Browning, T. J. and Moore, C. M.: Global analysis of ocean phytoplankton nutrient limitation reveals high prevalence of co-limitation, *Nat. Commun.*, 14, https://doi.org/10.1038/s41467-023-40774-0, 1775 2023.

Browning, T. J., Achterberg, E. P., Yong, J. C., Rapp, I., Utermann, C., Engel, A., and Moore, C. M.: Iron limitation of microbial phosphorus acquisition in the tropical North Atlantic, *Nat. Commun.*, 8, https://doi.org/10.1038/ncomms15465, 2017.

Buchanan, P. J., Aumont, O., Bopp, L., Mahaffey, C., and Tagliabue, A.: Impact of intensifying 1780 nitrogen limitation on ocean net primary production is fingerprinted by nitrogen isotopes, *Nat. Commun.*, 12, 6214, https://doi.org/10.1038/s41467-021-26552-w, 2021.

Caffin, M., Berthelot, H., Cornet-Barthaux, V., Barani, A., and Bonnet, S.: Transfer of diazotroph-derived nitrogen to the planktonic food web across gradients of N<sub>2</sub>/sub<sup>15</sup> fixation activity and diversity in the western tropical South Pacific Ocean, *Biogeosciences*, 15, 3795–3810, 1785 https://doi.org/10.5194/bg-15-3795-2018, 2018.

Casey, J. R., Mardinoglu, A., Nielsen, J., and Karl, D. M.: Adaptive Evolution of Phosphorus Metabolism in *Prochlorococcus*, *mSystems*, 1, e00065-16, https://doi.org/10.1128/mSystems.00065-16, 2016.

Cerdan-Garcia, E., Baylay, A., Polyviou, D., Woodward, E. M. S., Wrightson, L., Mahaffey, C., Lohan, M. C., Moore, C. M., Bibby, T. S., and Robidart, J. C.: Transcriptional responses of *Trichodesmium* to natural inverse gradients of Fe and P availability, *ISME J.*, 16, 1055–1064, https://doi.org/10.1038/s41396-021-01151-1, 2022.

Chappell, P. D., Moffett, J. W., Hynes, A. M., and Webb, E. A.: Molecular evidence of iron limitation and availability in the global diazotroph *Trichodesmium*, *ISME J.*, 6, 1728–1739, 1795 https://doi.org/10.1038/ismej.2012.13, 2012.

Chien, C., Mackey, K. R. M., Dutkiewicz, S., Mahowald, N. M., Prospero, J. M., and Paytan, A.: Effects of African dust deposition on phytoplankton in the western tropical Atlantic Ocean off Barbados, *Glob. Biogeochem. Cycles*, 30, 716–734, <https://doi.org/10.1002/2015gb005334>, 2016.

1800 Chisholm, S.W.: Phytoplankton size. Primary productivity and biogeochemical cycles in the sea, 213-237, 1992

Coleman, J. E.: Structure and Mechanism of Alkaline Phosphatase, *Annu. Rev. Biophys. Biomol. Struct.*, 21, 441–483, <https://doi.org/10.1146/annurev.bb.21.060192.002301>, 1992.

1805 Coutinho, F., Tschoeke, D. A., Thompson, F., and Thompson, C.: Comparative genomics of *Synechococcus* and proposal of the new genus *Parasynechococcus*, *PeerJ*, 4, e1522, <https://doi.org/10.7717/peerj.1522>, 2016.

Cox: Proteomic responses of oceanic *Synechococcus* WH8102 to phosphate and zinc scarcity and cadmium additions, *Front. Microbiol.*, <https://doi.org/10.3389/fmicb.2013.00387>, 2013.

1810 Davis, C. E., Blackbird, S., Wolff, G., Woodward, M., and Mahaffey, C.: Seasonal organic matter dynamics in a temperate shelf sea, *Prog. Oceanogr.*, 177, 101925, <https://doi.org/10.1016/j.pocean.2018.02.021>, 2019.

1815 Domínguez-Martín, M. A., López-Lozano, A., Melero-Rubio, Y., Gómez-Baena, G., Jiménez-Estrada, J. A., Kukil, K., Diez, J., and García-Fernández, J. M.: Marine *Synechococcus* sp. Strain WH7803 Shows Specific Adaptive Responses to Assimilate Nanomolar Concentrations of Nitrate, *Microbiol. Spectr.*, 10, <https://doi.org/10.1128/spectrum.00187-22>, 2022.

Duhamel, S., Diaz, J. M., Adams, J. C., Djaoudi, K., Steck, V., and Waggoner, E. M.: Phosphorus as an integral component of global marine biogeochemistry, *Nat. Geosci.*, 14, 359–368, <https://doi.org/10.1038/s41561-021-00755-8>, 2021.

1820 Edmonds, K. A., Jordan, M. R., and Giedroc, D. P.: COG0523 proteins: a functionally diverse family of transition metal-regulated G3E P-loop GTP hydrolases from bacteria to man, *Metallomics*, 13, <https://doi.org/10.1093/mtnmcs/mfab046>, 2021.

Grant, S. R., Church, M. J., Ferrón, S., Laws, E. A., and Rappé, M. S.: Elemental Composition, Phosphorous Uptake, and Characteristics of Growth of a SAR11 Strain in Batch and Continuous Culture, *mSystems*, 4, <https://doi.org/10.1128/msystems.00218-18>, 2019.

1825 Gross, A., Goren, T., Pio, C., Cardoso, J., Tirosh, O., Todd, M. C., Rosenfeld, D., Weiner, T., Custódio, D., and Angert, A.: Variability in Sources and Concentrations of Saharan Dust Phosphorus over the Atlantic Ocean, *Environ. Sci. Technol. Lett.*, 2, 31–37, <https://doi.org/10.1021/ez500399z>, 2015.

1830 Hawco, N. J., McIlvin, M. M., Bundy, R. M., Tagliabue, A., Goepfert, T. J., Moran, D. M., Valentín-Alvarado, L., DiTullio, G. R., and Saito, M. A.: Minimal cobalt metabolism in the marine cyanobacterium *Prochlorococcus*, *Proc. Natl. Acad. Sci.*, 117, 15740–15747, <https://doi.org/10.1073/pnas.2001393117>, 2020.

Held, N. A., Webb, E. A., McIlvin, M. M., Hutchins, D. A., Cohen, N. R., Moran, D. M., Kunde, K., Lohan, M. C., Mahaffey, C., Woodward, E. M. S., and Saito, M. A.: Co-occurrence of Fe and P stress in natural populations of the marine diazotroph *Trichodesmium*, *Biogeosciences*, 17, 2537–2551, <https://doi.org/10.5194/bg-17-2537-2020>, 2020.

1835 Held, N. A., Kunde, K., Davis, C. E., Wyatt, N. J., Mann, E. L., Woodward, E. M. S., McIlvin, M., Tagliabue, A., Twining, B. S., Mahaffey, C., Saito, M. A., and Lohan, M. C.: Part 2: Quantitative

contributions of cyanobacterial alkaline phosphatases to biogeochemical rates in the subtropical North Atlantic, <https://doi.org/10.5194/egusphere-2024-3996>, 4 March 2025.

1840 Hoppe, H. G.: Phosphatase activity in the sea, *Hydrobiologia*, 493, 187–200, <https://doi.org/10.1023/a:1025453918247>, 2003.

Ilikchyan, I. N., McKay, R. M. L., Kutowaya, O. A., Condon, R., and Bullerjahn, G. S.: Seasonal Expression of the Picocyanobacterial Phosphonate Transporter Gene *phnD* in the Sargasso Sea, *Front. Microbiol.*, 1, <https://doi.org/10.3389/fmicb.2010.00135>, 2010.

1845 Jakuba, R. W., Moffett, J. W., and Dyhrman, S. T.: Evidence for the linked biogeochemical cycling of zinc, cobalt, and phosphorus in the western North Atlantic Ocean, *Glob. Biogeochem. Cycles*, 22, <https://doi.org/10.1029/2007gb003119>, 2008.

Jickells, T. D.: The inputs of dust derived elements to the Sargasso Sea; a synthesis, *Mar. Chem.*, 68, 5–14, [https://doi.org/10.1016/s0304-4203\(99\)00061-4](https://doi.org/10.1016/s0304-4203(99)00061-4), 1999.

1850 Johnson, Z. I., Zinser, E. R., Coe, A., McNulty, N. P., Woodward, E. M. S., and Chisholm, S. W.: Niche Partitioning Among *Prochlorococcus* Ecotypes Along Ocean-Scale Environmental Gradients, *Science*, 311, 1737–1740, <https://doi.org/10.1126/science.1118052>, 2006.

Jones, R. D.: An improved fluorescence method for the determination of nanomolar concentrations of ammonium in natural waters, *Limnol. Oceanogr.*, 36, 814–819, <https://doi.org/10.4319/lo.1991.36.4.0814>, 1991.

1855 Kathuria, S. and Martiny, A. C.: Prevalence of a calcium-based alkaline phosphatase associated with the marine cyanobacterium *Prochlorococcus* and other ocean bacteria, *Environ. Microbiol.*, 13, 74–83, <https://doi.org/10.1111/j.1462-2920.2010.02310.x>, 2011.

1860 Kim, I.-N., Lee, K., Gruber, N., Karl, D. M., Bullister, J. L., Yang, S., and Kim, T.-W.: Increasing anthropogenic nitrogen in the North Pacific Ocean, *Science*, 346, 1102–1106, <https://doi.org/10.1126/science.1258396>, 2014.

Kunde, K., Wyatt, N. J., González-Santana, D., Tagliabue, A., Mahaffey, C., and Lohan, M. C.: Iron Distribution in the Subtropical North Atlantic: The Pivotal Role of Colloidal Iron, *Glob. Biogeochem. Cycles*, 33, 1532–1547, <https://doi.org/10.1029/2019GB006326>, 2019.

1865 Lapointe, B. E., Brewton, R. A., Herren, L. W., Wang, M., Hu, C., McGillicuddy, D. J., Lindell, S., Hernandez, F. J., and Morton, P. L.: Nutrient content and stoichiometry of pelagic Sargassum reflects increasing nitrogen availability in the Atlantic Basin, *Nat. Commun.*, 12, <https://doi.org/10.1038/s41467-021-23135-7>, 2021.

1870 Liang, Z., Letscher, R. T., and Knapp, A. N.: Dissolved organic phosphorus concentrations in the surface ocean controlled by both phosphate and iron stress, *Nat. Geosci.*, 15, 651–657, <https://doi.org/10.1038/s41561-022-00988-1>, 2022.

Liu, M., Matsui, H., Hamilton, D. S., Lamb, K. D., Rathod, S. D., Schwarz, J. P., and Mahowald, N. M.: The underappreciated role of anthropogenic sources in atmospheric soluble iron flux to the Southern Ocean, *Npj Clim. Atmospheric Sci.*, 5, <https://doi.org/10.1038/s41612-022-00250-w>, 2022.

1875 Lomas, M. W., Burke, A. L., Lomas, D. A., Bell, D. W., Shen, C., Dyhrman, S. T., and Ammerman, J. W.: Sargasso Sea phosphorus biogeochemistry: an important role for dissolved organic phosphorus (DOP), *Biogeosciences*, 7, 695–710, <https://doi.org/10.5194/bg-7-695-2010>, 2010.

1880 Lomas, M. W., Bonachela, J. A., Levin, S. A., and Martiny, A. C.: Impact of ocean phytoplankton diversity on phosphate uptake, Proc. Natl. Acad. Sci., 111, 17540–17545, <https://doi.org/10.1073/pnas.1420760111>, 2014.

1885 Lough, A. J. M., Homoky, W. B., Connelly, D. P., Comer-Warner, S. A., Nakamura, K., Abyaneh, M. K., Kaulich, B., and Mills, R. A.: Soluble iron conservation and colloidal iron dynamics in a hydrothermal plume, Chem. Geol., 511, 225–237, <https://doi.org/10.1016/j.chemgeo.2019.01.001>, 2019.

1890 Lu, X. and Zhu, H.: Tube-Gel Digestion, Mol. Cell. Proteomics, 4, 1948–1958, <https://doi.org/10.1074/mcp.m500138-mcp200>, 2005.

1895 Luo, H., Benner, R., Long, R. A., and Hu, J.: Subcellular localization of marine bacterial alkaline phosphatases, Proc. Natl. Acad. Sci., 106, 21219–21223, <https://doi.org/10.1073/pnas.0907586106>, 2009.

1900 Mahaffey, C., Reynolds, S., Davis, C. E., and Lohan, M. C.: Alkaline phosphatase activity in the subtropical ocean: insights from nutrient, dust and trace metal addition experiments, Front. Mar. Sci., 1, <https://doi.org/10.3389/fmars.2014.00073>, 2014.

1905 Mark Moore, C., Mills, M. M., Achterberg, E. P., Geider, R. J., LaRoche, J., Lucas, M. I., McDonagh, E. L., Pan, X., Poulton, A. J., Rijkenberg, M. J. A., Suggett, D. J., Ussher, S. J., and Woodward, E. M. S.: Large-scale distribution of Atlantic nitrogen fixation controlled by iron availability, Nat. Geosci., 2, 867–871, <https://doi.org/10.1038/ngeo667>, 2009.

1910 Martínez, A., Osburne, M. S., Sharma, A. K., DeLong, E. F., and Chisholm, S. W.: Phosphate utilization by the marine picocyanobacterium *Prochlorococcus* MIT9301, Environ. Microbiol., 14, 1363–1377, <https://doi.org/10.1111/j.1462-2920.2011.02612.x>, 2012.

1915 Martiny, A. C., Coleman, M. L., and Chisholm, S. W.: Phosphate acquisition genes in *Prochlorococcus* ecotypes: Evidence for genome-wide adaptation, Proc. Natl. Acad. Sci., 103, 12552–12557, <https://doi.org/10.1073/pnas.0601301103>, 2006.

1920 Martiny, A. C., Kathuria, S., and Berube, P. M.: Widespread metabolic potential for nitrite and nitrate assimilation among *Prochlorococcus* ecotypes, Proc. Natl. Acad. Sci., 106, 10787–10792, <https://doi.org/10.1073/pnas.0902532106>, 2009.

1925 McIlvin, M. R. and Saito, M. A.: Online Nanoflow Two-Dimension Comprehensive Active Modulation Reversed Phase–Reversed Phase Liquid Chromatography High-Resolution Mass Spectrometry for Metaproteomics of Environmental and Microbiome Samples, J. Proteome Res., 20, 4589–4597, <https://doi.org/10.1021/acs.jproteome.1c00588>, 2021.

1930 Menna, M.: Upwelling Features off the Coast of North-Western Africa in 2009-2013, BGTA, <https://doi.org/10.4430/bgta0164>, 2015.

1935 Mikhaylina, A., Ksibe, A. Z., Wilkinson, R. C., Smith, D., Marks, E., Coverdale, J. P. C., Fülöp, V., Scanlan, D. J., and Blidauer, C. A.: A single sensor controls large variations in zinc quotas in a marine cyanobacterium, Nat. Chem. Biol., 18, 869–877, <https://doi.org/10.1038/s41589-022-01051-1>, 2022.

1940 Mills, M. M., Ridame, C., Davey, M., La Roche, J., and Geider, R. J.: Iron and phosphorus co-limit nitrogen fixation in the eastern tropical North Atlantic, Nature, 429, 292–294, <https://doi.org/10.1038/nature02550>, 2004.

1945 Moore, C. M., Mills, M. M., Langlois, R., Milne, A., Achterberg, E. P., La Roche, J., and Geider, R. J.: Relative influence of nitrogen and phosphorous availability on phytoplankton physiology and

1920 productivity in the oligotrophic sub-tropical North Atlantic Ocean, *Limnol. Oceanogr.*, 53, 291–305, <https://doi.org/10.4319/lo.2008.53.1.0291>, 2008.

Moore, L., Ostrowski, M., Scanlan, D., Feren, K., and Sweetsir, T.: Ecotypic variation in phosphorus-acquisition mechanisms within marine picocyanobacteria, *Aquat. Microb. Ecol.*, 39, 257–269, <https://doi.org/10.3354/ame039257>, 2005.

1925 Nowicki, J. L., Johnson, K. S., Coale, K. H., Elrod, V. A., and Lieberman, S. H.: Determination of Zinc in Seawater Using Flow Injection Analysis with Fluorometric Detection, *Anal. Chem.*, 66, 2732–2738, <https://doi.org/10.1021/ac00089a021>, 1994.

Ostrowski, M., Mazard, S., Tetu, S. G., Phillippe, K., Johnson, A., Palenik, B., Paulsen, I. T., and Scanlan, D. J.: *PtrA* is required for coordinate regulation of gene expression during phosphate stress in a marine *Synechococcus*, *ISME J.*, 4, 908–921, <https://doi.org/10.1038/ismej.2010.24>, 2010.

1930 Painter, S., Sanders, R., Waldron, H., Lucas, M., and Torres-Valdes, S.: Urea distribution and uptake in the Atlantic Ocean between 50°N and 50°S, *Mar. Ecol. Prog. Ser.*, 368, 53–63, <https://doi.org/10.3354/meps07586>, 2008.

1935 Peñuelas, J., Poulter, B., Sardans, J., Ciais, P., Van Der Velde, M., Bopp, L., Boucher, O., Godderis, Y., Hinsinger, P., Llusia, J., Nardin, E., Vicca, S., Obersteiner, M., and Janssens, I. A.: Human-induced nitrogen–phosphorus imbalances alter natural and managed ecosystems across the globe, *Nat. Commun.*, 4, <https://doi.org/10.1038/ncomms3934>, 2013.

1940 Rapp, I., Schlosser, C., Rusiecka, D., Gledhill, M., and Achterberg, E. P.: Automated preconcentration of Fe, Zn, Cu, Ni, Cd, Pb, Co, and Mn in seawater with analysis using high-resolution sector field inductively-coupled plasma mass spectrometry, *Anal. Chim. Acta*, 976, 1–13, <https://doi.org/10.1016/j.aca.2017.05.008>, 2017.

Reistetter, E. N., Krumhardt, K., Callnan, K., Roache-Johnson, K., Saunders, J. K., Moore, L. R., and Rocap, G.: Effects of phosphorus starvation versus limitation on the marine cyanobacterium *Prochlorococcus* MED4 II: gene expression, *Environ. Microbiol.*, 15, 2129–2143, <https://doi.org/10.1111/1462-2920.12129>, 2013.

1945 Reynolds, S., Mahaffey, C., Roussenov, V., and Williams, R. G.: Evidence for production and lateral transport of dissolved organic phosphorus in the eastern subtropical North Atlantic, *Glob. Biogeochem. Cycles*, 28, 805–824, <https://doi.org/10.1002/2013gb004801>, 2014.

1950 Rodriguez, F., Lillington, J., Johnson, S., Timmel, C. R., Lea, S. M., and Berks, B. C.: Crystal Structure of the *Bacillus subtilis* Phosphodiesterase PhoD Reveals an Iron and Calcium-containing Active Site, *J. Biol. Chem.*, 289, 30889–30899, <https://doi.org/10.1074/jbc.m114.604892>, 2014.

Rouco, M., Frischkorn, K. R., Haley, S. T., Alexander, H., and Dyhrman, S. T.: Transcriptional patterns identify resource controls on the diazotroph *Trichodesmium* in the Atlantic and Pacific oceans, *ISME J.*, 12, 1486–1495, <https://doi.org/10.1038/s41396-018-0087-z>, 2018.

1955 Saito, M. A., Moffett, J. W., Chisholm, S. W., and Waterbury, J. B.: Cobalt limitation and uptake in *Prochlorococcus*, *Limnol. Oceanogr.*, 47, 1629–1636, <https://doi.org/10.4319/lo.2002.47.6.1629>, 2002.

Saito, M. A., McIlvin, M. R., Moran, D. M., Goepfert, T. J., DiTullio, G. R., Post, A. F., and Lamborg, C. H.: Multiple nutrient stresses at intersecting Pacific Ocean biomes detected by protein biomarkers, *Science*, 345, 1173–1177, <https://doi.org/10.1126/science.1256450>, 2014.

1960 Saito, M. A., Dorsk, A., Post, A. F., McIlvin, M. R., Rappé, M. S., DiTullio, G. R., and Moran, D. M.: Needles in the blue sea: Sub-species specificity in targeted protein biomarker analyses within the vast

oceanic microbial metaproteome, PROTEOMICS, 15, 3521–3531,  
<https://doi.org/10.1002/pmic.201400630>, 2015.

1965 Saito, M. A., Noble, A. E., Hawco, N., Twining, B. S., Ohnemus, D. C., John, S. G., Lam, P., Conway, T. M., Johnson, R., Moran, D., and McIlvin, M.: The acceleration of dissolved cobalt's ecological stoichiometry due to biological uptake, remineralization, and scavenging in the Atlantic Ocean, *Biogeosciences*, 14, 4637–4662, <https://doi.org/10.5194/bg-14-4637-2017>, 2017.

1970 Saito, M. A., Alexander, H., Benway, H., Boyd, P., Gledhill, M., Kujawinski, E., Levine, N., Maheigan, M., Marchetti, A., Obernosterer, I., Santoro, A., Shi, D., Suzuki, K., Tagliabue, A., Twining, B., and Maldonado, M.: The Dawn of the BioGeoSCAPES Program: Ocean Metabolism and Nutrient Cycles on a Changing Planet, *Oceanography*, 37, <https://doi.org/10.5670/oceanog.2024.417>, 2024.

1975 Scanlan, D. J., Mann, N. H., and Carr, N. G.: The response of the picoplanktonic marine cyanobacterium *Synechococcus* species WH7803 to phosphate starvation involves a protein homologous to the periplasmic phosphate-binding protein of *Escherichia coli*, *Mol. Microbiol.*, 10, 181–191, <https://doi.org/10.1111/j.1365-2958.1993.tb00914.x>, 1993.

1980 Sebastian, M. and Ammerman, J. W.: The alkaline phosphatase PhoX is more widely distributed in marine bacteria than the classical PhoA, *ISME J.*, 3, 563–572, <https://doi.org/10.1038/ismej.2009.10>, 2009.

1985 Sebastián, M., Arístegui, J., Montero, M. F., Escanez, J., and Xavier Niell, F.: Alkaline phosphatase activity and its relationship to inorganic phosphorus in the transition zone of the North-western African upwelling system, *Prog. Oceanogr.*, 62, 131–150, <https://doi.org/10.1016/j.pocean.2004.07.007>, 2004.

1990 Sohm, J. A., Mahaffey, C., and Capone, D. G.: Assessment of relative phosphorus limitation of *Trichodesmium* spp. in the North Pacific, North Atlantic, and the north coast of Australia, *Limnol. Oceanogr.*, 53, 2495–2502, <https://doi.org/10.4319/lo.2008.53.6.2495>, 2008.

1995 Srivastava, A., Saavedra, D. E. M., Thomson, B., García, J. A. L., Zhao, Z., Patrick, W. M., Herndl, G. J., and Baltar, F.: Enzyme promiscuity in natural environments: alkaline phosphatase in the ocean, *ISME J.*, 15, 3375–3383, <https://doi.org/10.1038/s41396-021-01013-w>, 2021.

1995 Steck, V., Lampe, R. H., Bhakta, S., Marrufo, K. C., Adams, J. C., Sachdev, E., Forsch, K. O., Barbeau, K. A., Allen, A. E., and Diaz, J. M.: Atypical phosphatases drive dissolved organic phosphorus utilization by phosphorus-stressed phytoplankton in the California Current Ecosystem, <https://doi.org/10.1101/2025.04.09.648040>, 9 April 2025.

1995 Su, B., Song, X., Duhamel, S., Mahaffey, C., Davis, C., Ivančić, I., and Liu, J.: A dataset of global ocean alkaline phosphatase activity, *Sci. Data*, 10, 205, <https://doi.org/10.1038/s41597-023-02081-7>, 2023.

2000 Sunda, W. G. and Huntsman, S. A.: Cobalt and zinc interreplacement in marine phytoplankton: Biological and geochemical implications, *Limnol. Oceanogr.*, 40, 1404–1417, <https://doi.org/10.4319/lo.1995.40.8.1404>, 1995.

2000 Tagliabue, A., Kwiatkowski, L., Bopp, L., Butenschön, M., Cheung, W., Lengaigne, M., and Vialard, J.: Persistent Uncertainties in Ocean Net Primary Production Climate Change Projections at Regional Scales Raise Challenges for Assessing Impacts on Ecosystem Services, *Front. Clim.*, 3, <https://doi.org/10.3389/fclim.2021.738224>, 2021.

Tarran, G. A., Heywood, J. L., and Zubkov, M. V.: Latitudinal changes in the standing stocks of nano- and picoeukaryotic phytoplankton in the Atlantic Ocean, *Deep Sea Res. Part II Top. Stud. Oceanogr.*, 53, 1516–1529, <https://doi.org/10.1016/j.dsr2.2006.05.004>, 2006.

2005 Tetu, S. G., Brahamsha, B., Johnson, D. A., Tai, V., Phillippy, K., Palenik, B., and Paulsen, I. T.: Microarray analysis of phosphate regulation in the marine cyanobacterium *Synechococcus* sp. WH8102, ISME J., 3, 835–849, <https://doi.org/10.1038/ismej.2009.31>, 2009.

2010 Torcello-Requesta, A., Murphy, A. R. J., Lidbury, I. D. E. A., Pitt, F. D., Stark, R., Millard, A. D., Puxty, R. J., Chen, Y., and Scanlan, D. J.: A distinct, high-affinity, alkaline phosphatase facilitates occupation of P-depleted environments by marine picocyanobacteria, Proc. Natl. Acad. Sci., 121, e2312892121, <https://doi.org/10.1073/pnas.2312892121>, 2024.

Ustick, L. J., Larkin, A. A., Garcia, C. A., Garcia, N. S., Brock, M. L., Lee, J. A., Wiseman, N. A., Moore, J. K., and Martiny, A. C.: Metagenomic analysis reveals global-scale patterns of ocean nutrient limitation, Science, 372, 287–291, <https://doi.org/10.1126/science.abe6301>, 2021.

2015 Van Mooy, B. A. S., Fredricks, H. F., Pedler, B. E., Dyhrman, S. T., Karl, D. M., Koblížek, M., Lomas, M. W., Mincer, T. J., Moore, L. R., Moutin, T., Rappé, M. S., and Webb, E. A.: Phytoplankton in the ocean use non-phosphorus lipids in response to phosphorus scarcity, Nature, 458, 69–72, <https://doi.org/10.1038/nature07659>, 2009.

2020 Welschmeyer, N. A.: Fluorometric analysis of chlorophyll a in the presence of chlorophyll b and pheophytins, Limnol. Oceanogr., 39, 1985–1992, <https://doi.org/10.4319/lo.1994.39.8.1985>, 1994.

White, A. E., Watkins-Brandt, K. S., Engle, M. A., Burkhardt, B., and Paytan, A.: Characterization of the Rate and Temperature Sensitivities of Bacterial Remineralization of Dissolved Organic Phosphorus Compounds by Natural Populations, Front. Microbiol., 3, <https://doi.org/10.3389/fmicb.2012.00276>, 2012.

2025 Wrightson, L. and Tagliabue, A.: Quantifying the Impact of Climate Change on Marine Diazotrophy: Insights From Earth System Models, Front. Mar. Sci., 7, 635, <https://doi.org/10.3389/fmars.2020.00635>, 2020.

2030 Yong, S. C., Roversi, P., Lillington, J., Rodriguez, F., Krehenbrink, M., Zeldin, O. B., Garman, E. F., Lea, S. M., and Berks, B. C.: A complex iron-calcium cofactor catalyzing phosphotransfer chemistry, Science, 345, 1170–1173, <https://doi.org/10.1126/science.1254237>, 2014.

Young, T. R., Martini, M. A., Foster, A. W., Glasfeld, A., Osman, D., Morton, R. J., Deery, E., Warren, M. J., and Robinson, N. J.: Calculating metalation in cells reveals CobW acquires CoII for vitamin B12 biosynthesis while related proteins prefer ZnII, Nat. Commun., 12, <https://doi.org/10.1038/s41467-021-21479-8>, 2021.

2035 Zinser, E. R., Johnson, Z. I., Coe, A., Karaca, E., Veneziano, D., and Chisholm, S. W.: Influence of light and temperature on Prochlorococcus ecotype distributions in the Atlantic Ocean, Limnol. Oceanogr., 52, 2205–2220, 2007.

Page 2: [1] Deleted	Claire Mahaffey	05/07/2025 07:03:00
---------------------	-----------------	---------------------

Page 2: [2] Deleted	Claire Mahaffey	13/06/2025 18:51:00
---------------------	-----------------	---------------------

Page 2: [3] Deleted	Claire Mahaffey	13/06/2025 18:53:00
---------------------	-----------------	---------------------

Page 2: [4] Commented [NH3]	Noelle Held	28/07/2025 10:11:00
-----------------------------	-------------	---------------------

I'm a little worried about this statement because it implies that there is a lot of P stress and that it is difficult to identify it, but the alternative is that there actually isn't a lot of P stress and that is why it is rarely found. We do point out some mechanisms that would make it more difficult to see P limitation (like biological plasticity) but those same mechanisms also exist for N and Fe.

Page 2: [5] Deleted	Claire Mahaffey	13/06/2025 18:54:00
---------------------	-----------------	---------------------

Page 15: [6] Deleted	Claire Mahaffey	05/07/2025 21:30:00
----------------------	-----------------	---------------------

Page 18: [7] Deleted	Noelle Held	28/07/2025 10:43:00
----------------------	-------------	---------------------

Page 18: [7] Deleted	Noelle Held	28/07/2025 10:43:00
----------------------	-------------	---------------------

Page 18: [8] Deleted	Claire Mahaffey	06/07/2025 20:04:00
----------------------	-----------------	---------------------

Page 18: [8] Deleted	Claire Mahaffey	06/07/2025 20:04:00
----------------------	-----------------	---------------------

Page 18: [8] Deleted	Claire Mahaffey	06/07/2025 20:04:00
----------------------	-----------------	---------------------

Page 18: [9] Deleted	Claire Mahaffey	06/07/2025 20:05:00
----------------------	-----------------	---------------------

Page 18: [9] Deleted	Claire Mahaffey	06/07/2025 20:05:00
----------------------	-----------------	---------------------

Page 18: [9] Deleted	Claire Mahaffey	06/07/2025 20:05:00
----------------------	-----------------	---------------------

Page 18: [10] Deleted	Noelle Held	28/07/2025 10:45:00
-----------------------	-------------	---------------------

Page 18: [10] Deleted	Noelle Held	28/07/2025 10:45:00
-----------------------	-------------	---------------------

Page 18: [11] Deleted	Claire Mahaffey	06/07/2025 20:21:00
▼		
▲		
Page 18: [11] Deleted	Claire Mahaffey	06/07/2025 20:21:00
▼		
▲		
Page 18: [11] Deleted	Claire Mahaffey	06/07/2025 20:21:00
▼		
▲		
Page 18: [11] Deleted	Claire Mahaffey	06/07/2025 20:21:00
▼		
▲		
Page 18: [12] Deleted	Claire Mahaffey	06/07/2025 20:24:00
▼		
▲		
Page 18: [12] Deleted	Claire Mahaffey	06/07/2025 20:24:00
▼		
▲		
Page 18: [13] Deleted	Claire Mahaffey	06/07/2025 20:22:00
▼		
▲		
Page 18: [13] Deleted	Claire Mahaffey	06/07/2025 20:22:00
▼		
▲		
Page 18: [14] Deleted	Claire Mahaffey	06/07/2025 20:25:00
▼		
▲		
Page 18: [14] Deleted	Claire Mahaffey	06/07/2025 20:25:00
▼		
▲		
Page 18: [14] Deleted	Claire Mahaffey	06/07/2025 20:25:00
▼		
▲		
Page 18: [14] Deleted	Claire Mahaffey	06/07/2025 20:25:00
▼		
▲		
Page 18: [15] Deleted	Noelle Held	28/07/2025 10:46:00
▼		
▲		
Page 18: [16] Deleted	Claire Mahaffey	06/07/2025 20:39:00
▼		
▲		
Page 18: [16] Deleted	Claire Mahaffey	06/07/2025 20:39:00
▼		
▲		
Page 18: [16] Deleted	Claire Mahaffey	06/07/2025 20:39:00
▼		
▲		
Page 18: [16] Deleted	Claire Mahaffey	06/07/2025 20:39:00
▼		
▲		
Page 18: [16] Deleted	Claire Mahaffey	06/07/2025 20:39:00

▼  
▲ **Page 18: [16] Deleted** Claire Mahaffey **06/07/2025 20:39:00**

▼  
▲ **Page 18: [16] Deleted** Claire Mahaffey **06/07/2025 20:39:00**

▼  
▲ **Page 18: [17] Deleted** Claire Mahaffey **06/07/2025 20:41:00**

▼  
▲ **Page 18: [17] Deleted** Claire Mahaffey **06/07/2025 20:41:00**

▼  
▲ **Page 18: [17] Deleted** Claire Mahaffey **06/07/2025 20:41:00**

▼  
▲ **Page 18: [17] Deleted** Claire Mahaffey **06/07/2025 20:41:00**

▼  
▲ **Page 18: [17] Deleted** Claire Mahaffey **06/07/2025 20:41:00**

▼  
▲ **Page 18: [17] Deleted** Claire Mahaffey **06/07/2025 20:41:00**

▼  
▲ **Page 18: [17] Deleted** Claire Mahaffey **06/07/2025 20:41:00**

▼  
▲ **Page 18: [17] Deleted** Claire Mahaffey **06/07/2025 20:41:00**

▼  
▲ **Page 18: [17] Deleted** Claire Mahaffey **06/07/2025 20:41:00**

▼  
▲ **Page 18: [18] Formatted** Claire Mahaffey **30/06/2025 08:00:00**

Font: Not Italic  
▲ **Page 18: [18] Formatted** Claire Mahaffey **30/06/2025 08:00:00**

Font: Not Italic  
▲ **Page 18: [18] Formatted** Claire Mahaffey **30/06/2025 08:00:00**

Font: Not Italic  
▲ **Page 18: [18] Formatted** Claire Mahaffey **30/06/2025 08:00:00**

Font: Not Italic  
▲ **Page 18: [18] Formatted** Claire Mahaffey **30/06/2025 08:00:00**

Font: Not Italic  
▲

Page 18: [19] Deleted	Claire Mahaffey	30/06/2025 08:00:00
▼		
Page 18: [19] Deleted	Claire Mahaffey	30/06/2025 08:00:00
▼		
Page 18: [19] Deleted	Claire Mahaffey	30/06/2025 08:00:00
▼		
Page 18: [19] Deleted	Claire Mahaffey	30/06/2025 08:00:00
▼		
Page 18: [20] Formatted	Noelle Held	28/07/2025 10:47:00
Font: Italic		
Page 18: [20] Formatted	Noelle Held	28/07/2025 10:47:00
Font: Italic		
Page 18: [21] Deleted	Claire Mahaffey	07/07/2025 05:39:00
▼		
Page 18: [21] Deleted	Claire Mahaffey	07/07/2025 05:39:00
▼		
Page 20: [22] Deleted	Claire Mahaffey	06/07/2025 06:59:00
Page 21: [23] Deleted	Claire Mahaffey	07/07/2025 06:44:00
Page 21: [24] Deleted	Claire Mahaffey	07/07/2025 07:20:00
▼		